day 550 in patient 2. Although the MPA AUC_{0-12h} decreased to 15.3 $\mu g \cdot h \cdot ml^{-1}$ on day 370, the high CsA AUC_{0-4h} (4,204 $ng \cdot h \cdot ml^{-1}$) and C_2 (1,452 ng/ml) were maintained, which may have prevented acute rejection in patient 2. Patient 3 did not experience acute rejection during the MMF washout period from day 99 to day 262, which may be attributed to the high AUC_{0-4h} (4,019 $ng \cdot h \cdot ml^{-1}$) or C_2 (1,249 ng/ml). These findings suggest that the high CsA AUC_{0-4h} (>4,000 $ng \cdot h \cdot ml^{-1}$) or C_2 (>1,200 ng/ml) might prevent acute rejection, even if the MPA AUC_{0-12h} is 30 $\mu g \cdot h \cdot ml^{-1}$ or less.

We calculate the AUC of CsA in heart transplant patients who are admitted for myocardial biopsy and monitor the C_0 and C_2 levels (the reference levels) of outpatients to determine the dose of CsA. However, there was no clear link between the risk of acute rejection and CsA C_0 levels in these 3 patients. It has been reported that, in determining the appropriate dose, monitoring of the absorption profile is more important than conventional C_0 monitoring of CsA.[4–8] The AUC_{0-4h} is the important parameter of the absorption profile; however, a 1-point monitoring strategy needs to be developed for predicting the AUC_{0-4h} in clinical practice, in particular for outpatients.[22] It has been reported that C_2 is the most accurate surrogate marker for AUC_{0-4h},[4–6] and has been found to be a better marker for rejection and nephrotoxicity than C_0.[4,5] Our experience also suggests that the CsA C_2 values changed in relation to the AUC_{0-4h}. Cantarovich et al[6,9,23] report a clinical benefit of CsA C_2 monitoring (as opposed to C_0 monitoring) in long-term heart transplant patients. The C_2 target levels of their study were as follows: 0–3 months, 600–800 ng/ml; 4–6 months, 500–700 ng/ml; >6 months, 400–600 ng/ml. Other groups report that high C_2 values (1,015±422 ng/ml) are associated with fewer episodes of acute cellular rejection in patients who have undergone heart transplantation;[10] and that acute cellular rejection should be suspected when the C_2 level is below 600 ng/ml.[6,11] At present, at the NCVC, the AUC_{0-4h} is predicted from C_0 and C_2, which are monitored in outpatients to determine the dose of CsA. However, the appropriate target value for either the AUC_{0-4h} or C_2 of CsA in heart transplant recipients is not fixed.

On the other hand, the target AUC_{0-12h} value for MPA after heart transplantation has been reported to be 30–60 $\mu g \cdot h \cdot ml^{-1}$.[13] In addition, the 3-point monitoring of C_0, $C_{0.5}$, and C_2 has been reported to be highly correlated with the AUC_{0-12h}.[24]

We demonstrated that a high CsA AUC_{0-4h} may help prevent cardiac allograft rejection in patients who temporarily stop MMF treatment. When MMF is stopped or drastically reduced, the dose of CsA should be increased to maintain the high CsA AUC_{0-4h} (>4,000 $ng \cdot h \cdot ml^{-1}$). Although our study had a limited number of patients, it is the first to characterize the relationship between acute rejection and either the CsA or MPA level in heart transplant recipients. Further studies should be conducted to investigate the relationship between the CsA AUC_{0-4h} or MPA AUC_{0-12h} and the risk of rejection, and the effectiveness of CsA C_2 monitoring in heart transplant patients should be confirmed.

References

1. Nakatani T. The present status of heart transplantation in Japanese. *Transplant Now* 2005; 18: 287–293.
2. Kitamura S, Kurosawa H, Kondo T, Simizu N, Matuda H, Wada H. Heart and lung transplantation protocols. First ed, Medical View Company, Japan, 2003.
3. Belitsky P, Dunn S, Johnston A, Levy G. Impact of absorption profiling on efficacy and safety of cyclosporin therapy in transplant recipients. *Clin Pharmacokinet* 2000; 39: 117–125.
4. Mahalati K, Belitsky P, Sketris I, West K, Panek R. Neoral monitoring by simplified sparse sampling area under the concentration-time curve: Its relationship to acute rejection and cyclosporine nephrotoxicity early after kidney transplantation. *Transplantation* 1999; 68: 55–62.
5. Belitsky P, Levy GA, Johnston A. Neoral absorption profiling: An evolution in effectiveness. *Transplant Proc* 2000; 32: 45S–52S.
6. Cantarovich M, Elstein E, de Varennes B, Barkun JS. Clinical benefit of Neoral dose monitoring with cyclosporine 2-hr post-dose levels compared with trough levels in stable heart transplant patients. *Transplantation* 1999; 68: 1839–1842.
7. Armstrong VW, Oellerich M. New developments in the immunosuppressive drug monitoring of cyclosporine, tacrolimus, and azathioprine. *Clin Biochem* 2001; 34: 9–16.
8. Cooney GF, Johnston A. Neoral C-2 monitoring in cardiac transplant patients. *Transplant Proc* 2001; 33: 1572–1575.
9. Cantarovich M, Besner JG, Barkun JS, Elstein E, Loertscher R. Two-hour cyclosporine level determination is the appropriate tool to monitor Neoral therapy. *Clin Transplant* 1998; 12: 243–249.
10. Delgado DH, Rao V, Hamel J, Miriuka S, Cusimano RJ, Ross HJ. Monitoring of cyclosporine 2-hour post-dose levels in heart transplantation: Improvement in clinical outcomes. *J Heart Lung Transplant* 2005; 24: 1343–1346.
11. Chou NK, Chen RJ, Ko WJ, Lin HL, Yu SY, Chen YS, et al. Cyclosporine C2 monitoring is superior to C0 in predicting acute cellular rejection in heart transplant recipients in Taiwan. *Transplant Proc* 2004; 36: 2393–2395.
12. Shaw LM, Nicholls A, Hale M, Armstrong VW, Oellerich M, Yatscoff R, et al. Therapeutic monitoring of mycophenolic acid: A consensus panel report. *Clin Biochem* 1998; 31: 317–322.
13. DeNofrio D, Loh E, Kao A, Korecka M, Pickering FW, Craig KA, et al. Mycophenolic acid concentrations are associated with cardiac allograft rejection. *J Heart Lung Transplant* 2000; 19: 1071–1076.
14. Shaw LM, Korecka M, Aradhye S, Grossman R, Bayer L, Innes C, et al. Mycophenolic acid area under the curve values in African American and Caucasian renal transplant patients are comparable. *J Clin Pharmacol* 2000; 40: 624–633.
15. Barten MJ, Rahmel A, Garbade J, Richter M, Bittner HB, Dhein S, et al. C0h/C2h monitoring of the pharmacodynamics of cyclosporin plus mycophenolate mofetil in human heart transplant recipients. *Transplant Proc* 2005; 37: 1360–1361.
16. Hale MD, Nicholls AJ, Bullingham RE, Hene R, Hoitsma A, Squifflet JP, et al. The pharmacokinetic-pharmacodynamic relationship for mycophenolate mofetil in renal transplantation. *Clin Pharmacol Ther* 1998; 64: 672–683.
17. Takahashi K, Ochiai T, Uchida K, Yasumura T, Ishibashi M, Suzuki S, et al. Pilot study of mycophenolate mofetil (RS-61443) in the prevention of acute rejection following renal transplantation in Japanese patients: RS-61443 Investigation Committee Japan. *Transplant Proc* 1995; 27: 1421–1424.
18. Shaw LM, Korecka M, DeNofrio D, Brayman KL. Pharmacokinetic, pharmacodynamic, and outcome investigations as the basis for mycophenolic acid therapeutic drug monitoring in renal and heart transplant patients. *Clin Biochem* 2001; 34: 17–22.
19. Shaw LM, Kaplan B, DeNofrio D, Korecka M, Brayman KL. Pharmacokinetics and concentration-control investigations of mycophenolic acid in adults after transplantation. *Ther Drug Monit* 2000; 22: 14–19.
20. Tsina I, Kaloostian M, Lee R, Tarnowski T, Wong B. High-perfomance liquid chromatographic method for the determination of mycophenolate mofetil in human plasma. *J Chromatogr B Biomed Appl* 1996; 68: 347–353.
21. Monta O, Matsumiya G, Fukushima N, Miyamoto Y, Sawa Y, Koseki M, et al. Mechanical ventricular assist system required for sustained severe cardiac dysfunction secondary to peripartum cardiomyopathy. *Circ J* 2005; 69: 362–364.
22. Wada K, Takada M, Ueda T, Ochi H, Morishita H, Hanatani A, et al. Pharmacokinetic study and limited sampling strategy of cyclosporine in Japanese heart transplant recipients. *Circ J* 2006; 70: 1307–1311.
23. Cantarovich M, Giannetti N, Cecere R. Impact of cyclosporine 2-h level and Mycophenolate mofetil dose on clinical outcomes in de novo heart transplant patients receiving anti-thymocyte globulin induction. *Clin Transplant* 2003; 17: 144–150.
24. Pawinski T, Hale M, Korecka M, Fitzsimmons WE, Shaw LM. Limited sampling strategy for the estimation of Mycophenolic acid area under the curve in adult renal transplant patients treated with concomitant tacrolimus. *Clin Chem* 2002; 48: 1497–1504.

Circ J 2004; **68:** 677–682

Identification of Autoantibodies With the Corresponding Antigen for Repetitive Coxsackievirus Infection-Induced Cardiomyopathy

Satoko Takata, MD; Hiroshi Nakamura, MD; Seiji Umemoto, MD; Kazuhito Yamaguchil, DVM*; Taichi Sekine, MSc**; Tomohiro Kato, MD**; Kusuki Nishioka, MD**; Masunori Matsuzaki, MD

Background The hypothesis that viral myocarditis causes an autoimmune response and subsequent dilated cardiomyopathy is controversial. To further investigate the autoimmune mechanism of cardiac dilatation and dysfunction after repeated episodes of viral myocarditis, the cardiac autoantigens induced by repetitive coxsackievirus B3 (CVB3) infection were examined.

Methods and Results Male inbred A/J mice were inoculated intraperitoneally with CVB3 at 3 and 40 weeks of age. At 8 weeks after the second inoculation, the mortality of the repetitive CVB3 group was significantly increased compared with that of the control group, and was associated with a significant reduction in fractional shortening and marked left ventricular dilatation without inflammatory cell infiltration. The cardiac antigens in the repetitive CVB3 infection were identified by 2-dimensional electrophoresis and subsequent liquid chromatography/tandem mass spectrometry (LC-MS/MS) using the serum at 2 weeks after the second inoculation. LC-MS/MS and immunohistochemistry demonstrated α-cardiac actin and heat shock protein 60 (HSP60) as cardiac near-surface antigens induced by the repetitive CVB3 infection. Immunoelectron microscopy disclosed the selective localization of anti-IgM antibody on the membrane of the myocytes in the repetitive CVB3 group.

Conclusions IgM antibodies against α-cardiac actin and HSP60, which were induced by repetitive CVB3 infection, may play an important role in the pathophysiology of the subsequent cardiac dysfunction and dilatation. (*Circ J* 2004; **68:** 677–682)

Key Words: Autoantigen; Autoimmunity; Coxsackievirus; HSP60; Viral Myocarditis

Dilated cardiomyopathy (DCM) is characterized by the dilatation and impaired contraction of the ventricles and clinically progressive heart failure[1] It may be idiopathic, familial/genetic, viral and/or immune, alcoholic/toxic, or associated with recognized cardiovascular disease in which the degree of myocardial dysfunction is not explained by the abnormal loading conditions or the extent of ischemic damage. Although the relationship between viral myocarditis and DCM remains controversial, a causal link has become more evident because of the tremendous developments in the molecular analyses of autopsy and endomyocardial biopsy specimens, new techniques of viral gene amplification, and advances in modern immunology[2,3]

It has already been reported that an autoimmune response plays a key role in the progression after viral myocarditis[3,4] This occurs in the context of a polyclonal stimulation of the immune system after the initial viral assault that may have been already cleared when the autoreactive B- and T-cell response occurs[5] Recently, we demonstrated that repetitive coxsackievirus B3 (CVB3) infection produced cardiac dilatation without inflammatory cell infiltration in the heart of mice with post-myocarditis, and autoimmunity mediated by the circulation of certain antibodies (eg, antibodies against the CVB3 genome or a CVB3-related protein) may be part of the pathogenic mechanism for this phenomenon. Moreover, only the autoreactive IgM antibody was apparent on the cell membrane of the myocytes and interstitial tissue in the repetitive infected mice, and may play a pivotal role in the early response to the virus in our repetitive viral myocarditic mice[6] To identify the autoantigen against the components of the myocardium in repetitive CVB3 myocarditic mice, particularly targeting the cell membrane, we examined whether IgM type-autoantibodies were present in the serum of these animals.

Methods

The experimental protocols used in this study were approved by the Ethics Committee for Animal Experimentation at Yamaguchi University School of Medicine, and carried out according to the Guidelines for Animal Experimentation at Yamaguchi University School of Medicine, and Law No. 105 and Notification No. 6 of the Japanese Government.

(Received November 28, 2003; revised manuscript received April 27, 2004; accepted April 30, 2004)

*Department of Cardiovascular Medicine and *Institute of Laboratory Animals, Yamaguchi University Graduate School of Medicine, Ube, and **Division of Rheumatology, Immunology and Genetics Program, Institute of Medical Science, St Marianna University School of Medicine, Kawasaki, Japan*

Mailing address: Masunori Matsuzaki, MD, PhD, Department of Cardiovascular Medicine, Yamaguchi University Graduate School of Medicine, 1-1-1 Minami Kogushi, Ube, Yamaguchi 755-8505, Japan. E-mail: ninai@yamaguchi-u.ac.jp

Experimental Protocol

Three-week old, inbred, certified, virus-free A/J (H-2a) male mice were purchased from Japan SLC (Shizuoka, Japan). Fourteen normal mice were also housed for 40 weeks as a control (3W–/40W–). The CVB3 (Nancy strain) was obtained from the American Type Culture Collection and stored at –80°C until use. Each 3-week old mouse was initially infected by an intraperitoneal injection of 2×10^4 plaque-forming units of CVB3 in 0.2 ml of saline. The infected mice were isolated, 5 per cage, in a special unit for 37 weeks (3W+/40W–). A total of 31 mice first inoculated at 3 weeks were reinfected in the same manner with CVB3 at 40 weeks (3W+/40W+). In addition, 5 normal mice were inoculated at 40 weeks (3W–/40W+) as a further control group. At 8 weeks after reinfection, the mice were weighed and killed with KCl injection via the inferior vena cava to stop the heart in end-diastole. Body weight was measured, and the hearts, lungs, and livers were excised and weighed. The control mice were treated in the same manner, but with saline that did not contain the virus.

Morphometry and Histopathological Study

The ventricles from the mice killed at 8 weeks after the second inoculation were halved transversely and one portion was fixed with 10% formalin solution, then embedded in paraffin solution and sectioned into slices of 4-mm thickness stained with hematoxylin-eosin and Azan solutions. The left ventricular (LV) dimensions and wall thickness were measured using the transverse section of the middle portion of the ventricle. The cavity dimensions and wall thickness of the left ventricle were calculated according to the method of Matsumori et al[7] Cardiac fibrosis was also evaluated quantitatively using a Fotovision FV-10 camera (Fuji Film Co, Japan) and a (Macintosh 8500/120) computer equipped with NIH Image version 1.62 software.

Echocardiography

Prior to death at 8 weeks after the second inoculation, the mice underwent light anesthesia with ether. The LV end-diastolic dimension (EDD), end-systolic dimension (ESD), and fractional shortening (%FS) were obtained by averaging the data from 3 cardiac cycles using an echocardiographic system (ALOKA 5500; Aloka, Japan) with a dynamically focused 10-MHz linear array transducer.

Immunoelectron Microscopy

Immunoelectron microscopy was performed by the method of Yamaguchi et al[8] Briefly, the hearts at 2 weeks after the second inoculation were fixed by perfusing with paraformaldehyde. For immunostaining, horseradish peroxidase (HRP) conjugated anti-mouse IgM was used. Sections 10–19 nm thick were examined with a JEOL 200 CX transmission electron microscope at 160 kV. Sarcomere lengths were measured in a blinded fashion at a magnification of 3,700. This process was repeated for 50 fields per animal.

Two-Dimensional Western Blotting

Fresh murine heart tissue at 2 weeks after the second inoculation was minced and resuspended in 5 volumes of STE buffer containing 320 mmol/L sucrose, 10 mmol/L Tris–HCl, pH 7.4, 1 mmol/L EGTA, 5 mmol/L NaN3, 10 mmol/L -mercaptoethanol, 20 mmol/L leupeptin, 0.15 mmol/L pepstatin A, 0.2 mmol/L phenylmethylsulfonyl fluoride, and 50 mmol/L NaF, with a Polytron homogenizer (PT1200; Kinematica, Germany), at its maximum speed for 30 s, repeated 3 times. Homogenates were mixed with an equal volume of STE buffer and centrifuged at 1,000 G for 10 min, and the supernatant was centrifuged at 100,000 G for 60 min. The 1,000-G and 100,000-G pellets were designated as P1 and P2 fractions, respectively, and the 100,000-G supernatant as the S fraction. The P1 and P2 fractions were resuspended in STE buffer. The total protein concentration in each fraction was determined, using bovine serum albumin as a standard[9]

The extracted protein samples were diluted in a rehydration buffer (8 mol/L urea, 2% CHAPS, 2.8 mg/ml dithiothreitol (DTT), trace of bromphenol blue) containing 0.5% immobilized pH gradient (IPG) buffer (pH range 3–10; Amersham Pharmacia Biotech, Sweden), and loaded onto 7 cm Immobiline Drystrips (Amersham Pharmacia Biotech) in the IPG reswelling tray (Amersham Pharmacia Biotech) at room temperature overnight. Up to 400 mg of the extracted proteins was applied onto the drystrip gels for western blotting, and up to 1,000 mg for the analysis by mass spectrometry. Isoelectric focusing (IEF) was performed in a horizontal electrofocusing apparatus (MultiPhor II; Pharmacia Biotech, Sweden) according to the manufacturer's instructions. After the IEF, the IPG strips were equilibrated in 2 equilibration solutions. The first equilibration solution consisted of 10 mg DTT per 1 ml sodium dodecyl sulfate (SDS) equilibration buffer (1.5 mol/L Tris-Cl, pH8.8; 6 mol/L urea, 30% glycerol, 2% SDS), and the second equilibration solution consisted of 25 mg iodoacetamide per 1 ml SDS equilibration buffer. The equilibrated strips were placed on top of a 12.5% SDS polyacrylamide gel electrophoresis (PAGE) slab and sealed with 0.5% lower melt gel, and then the second electrophoresis was performed with a 40 mA constant current in the separating gel at 20°C.

After electrophoresis, the SDS-PAGE gels were stained with Coomassie Brilliant Blue (CBB) or used for protein transfer onto nitrocellulose membranes (Protran, Schleicher & Schuell, Germany). In the western blotting, the membranes were blocked in phosphate-buffered saline (PBS) containing 1% bovine serum albumin (BSA) and 0.1% Tween 20 for 1 h, washed in PBS with 0.1% Tween 20 (PBST) for 30 min, and incubated with serum samples, which were collected from mice at 2 weeks after the second inoculation, diluted adequately in PBST containing 1% BSA for 1 h. After 5 washings in PBST, the bound antibodies were reacted with HRP-conjugated goat anti-mouse IgM (Sigma, St Louis, MO, USA) for 1 h. Finally, the bound antibodies were visualized by diaminobenzidine.

Mass Determination and Mass Fingerprinting

Liquid chromatography/tandem mass spectrometry (LC-MS/MS) was performed as follows to determine the molecular weight of the protein spots. Protein spots on the gel stained with CBB, which corresponded to the positive spots on the western blotting membranes, were recovered and then the recovered gel fragments were washed in double distilled water for 15 min, de-colored in 50 ml decoloring solution (0.1 mol/L ammonium hydrogen carbonate, 50% methanol) at 40°C for 15 min, and cut into small pieces. The gel pieces were re-hydrated in 20 ml trypsin solution (0.1 pmol/ml trypsin in 50 mmol/L Tris-HCl; Wako Pure Chemical Industries, Ltd, Japan) and incubated at 37°C. The digested peptides were extracted from the gel pieces using trifluoroacetic acid (TFA) and acetonitrile.

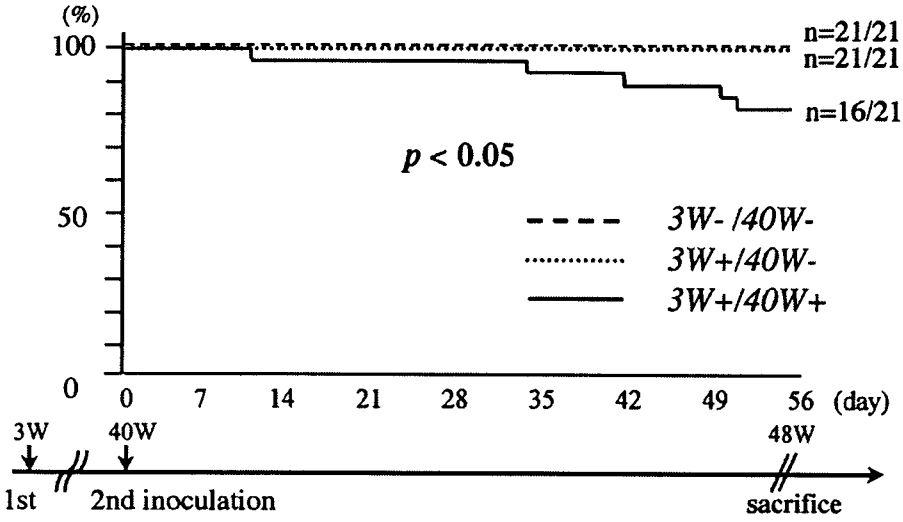

Fig 1. Survival curve after the second inoculation in viral myocarditic mice at 40 weeks. A survival reduction of 23.8% was observed in the repetitive group (3W+/40W+) compared with the control group (3W–/40W–) at 8 weeks after the second inoculation. *p<0.05 vs both the 3W–/40W– and 3W+/40W– groups. No mice died after the second vehicle injection.

Specifically, the digested products were added to 50 ml of 0.1% TFA/50% acetonitrile, vortexed, and sonicated for 10 min. After centrifugation, the supernatant was recovered. After 2 more cycles of this extraction, a similar extraction was performed with 50 ml of 0.1% TFA/80% acetonitrile. The collected supernatant was centrifuged again, filtered, and concentrated down to 50 ml in an evaporator, and was then desalted using a Zip-Tip desalting column (Millipore Corp, Milford, MA, USA). The peptide sample solution was stored at –20°C until mass spectrometry analysis.

The mass of the digested peptides in the samples was determined using a mass spectrometer with matrix-assisted laser desorption/ionization-time of flight (MALDI-TOF: Voyager DE-STR; PerSeptive Biosystems, USA). Alpha-cyano-4-hydroxycinnamic acid was used as an assisting matrix. A list of the determined peptide masses was made by a mass fingerprint search of the NCBI protein databases using the Mascot software program (Matrix Science, Ltd, UK), in which the NCBI protein databases were searched.

Immunohistochemistry

For immunoenzymatic staining, the remaining ventricular portion was quickly frozen with OCT compound (Miles, Inc, USA) in liquid nitrogen and stored at –80°C. The frozen specimens were sectioned at 4-mm thickness. Immunoenzymatic staining was performed with a DAKO LSAB kit (DAKO, USA) according to the manufacturer's instructions. Antibody against murine heart shock protein 60 (HSP60) (Stressgen, Canada) was used as the primary antibody.

Statistical Analysis

Data were expressed as the mean ± SD. Statistical analysis of the data was performed by an analysis of variance with multiple comparisons. The survival of all animals was assessed by Kaplan-Meier analysis. A level of $p<0.05$ was considered statistically significant.

Results

Survival Rates

Fig 1 shows the survival curve at 8 weeks after the second inoculation at 40 weeks. Five of the 21 mice died after the second CVB3 inoculation (mortality rate: 23.8%, $p<0.05$). All of the dead mice had pleural effusion and ascites, indicating that they probably died from heart failure. No mice died after the second vehicle injection.

Table 1 Assessment of the Systemic Parameters of Viral Myocarditis

	Group		
	3W–/40W–	3W+/40W–	3W+/40W+
Physiological analysis			
No. of experiments	5	5	5
Body weight (g)	29.2±2.8	30.2±2.5	26.3±2.0†
Heart weight (mg)	108±4.2	140.8±38.4	201.4±91.0*
Lung weight (mg)	212±3.6	199±92	221±93
Liver weight (mg)	1,173±268	1,023±101	967±4
HW/BW(mg/g)	3.73±0.45	4.65±1.11	7.89±4.15*
LW/BW (mg/g)	7.25±0.90	6.55±2.75	8.5±4.38
LIW/BW (mg/g)	40.21±8.31	34.21±2.44	36.28±1.99
Morphometry			
Wall thickness (mm)	0.8±0.1	0.7±0.1	0.7±0.1
Fibrosis (%)	3.1±0.7	16.5±11.1*	26.9±6.0*†
Inflammatory grading	0	0.2±0.4	0.2±0.4
Echocardiography			
LVEDD (mm)	2.4±0.3	2.6±0.4	3.4±0.3*†
LVESD (mm)	0.9±0.1	1.3±0.3*	2.4±0.5*†
%FS (%)	60.8±5.4	50.6±7.6*	29.6±7.9*

HW/BW, ratio of heart weight/body weight; LW/BW, ratio of lung weight/body weight; LIW/BW, ratio of liver weight/body weight; LVEDD, left ventricular end-diastolic dimension; LVESD, left ventricular end-systolic dimension; %FS, fractional shortening.
*Values are the mean ± SD. *p<0.05 vs the 3W–/40W– group. †p<0.05 vs the 3W+/40W– group.*

Physiological Analysis

The mean body weight in the 3W+/40W+ group was significantly reduced compared with that in the 3W+/40W– group ($p<0.05$). The heart weight and the ratio of heart weight/body weight in the 3W+/40W+ group was significantly increased compared with that in the 3W–/40W– group ($p<0.05$) (Table 1). There were no differences between the 3W–/40W– and 3W+/40W– groups in body weight or heart weight, or in the ratio of the heart weight/body weight. In addition, there were no significant differences in the weights of the lungs and livers among the 3 groups.

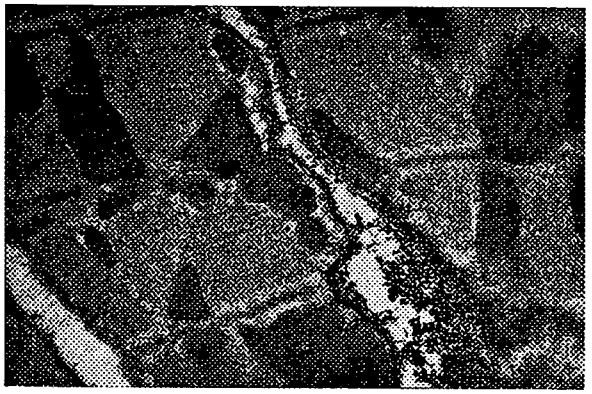

Fig 2. Ultrastructural localization of anti-heart antibodies was confirmed on the surface of the myocytes and interstitial tissue with immunoelectron microscopy (×10,000).

Histology

There was a significant increase in the LV dimension in the 3W+/40W+ group compared with the 3W+/40W− group ($p<0.05$). The ratio of cardiac fibrosis in the 3W+/40W− and 3W+/40W+ groups was significantly higher than in the 3W−/40W− group ($p<0.05$). The ratio of cardiac fibrosis in the 3W+/40W+ group was the highest among the 3 groups (Table 1). There was no significant difference in the mean wall thickness among the 3 groups. Inflammatory cell infiltration was less than 5% in all groups (Table 1).

Echocardiography

To evaluate cardiac function, we performed transthoracic echocardiography at 8 weeks after the second inoculation. Both the LVEDD and LVESD of the 3W+/40W+ group were significantly increased compared with those of the other 2 groups; %FS was significantly reduced in the 3W+/40W+ group compared with that in the other 2 groups (Table 1).

Immunoelectron Microscopy

The sarcomere length in the 3W+/40W+ group was 1.8±0.24 mm, which is comparable to the data previously obtained[6] Staining of bound IgM in the myocardium was recognized only in the 3W+/40W+ group. The cell membranes of the myocytes and interstitial tissue were positively stained with the anti-IgM antibody by immunoelectron microscopy (Fig 2).

Two-Dimensional Western Blotting and Subsequent LC-MS/MS

On 2-dimensional western blotting, 2 spots were detected as A3 (pI 5.2) and A5 (pI 5.9) in the membranous fraction that specifically cross-reacted with the serum in the 3W+/40W+ group (Fig 3). By subsequent LC-MS/MS, A3 (MW 42001 Da) and A5 (MW 60941 Da) were recognized as a-cardiac actin and HSP60, respectively (Fig 3).

Immunohistochemistry

Because α-cardiac actin is known to be ubiquitously distributed in myocytes, and only HSP60 is reported to be upregulated on the cell surface, as well as in the cytosol and mitochondria in response to many different stresses,[10] we performed further immunohistochemical analysis for HSP60 at 2 weeks after the second inoculation. We showed that HSP60 was positively stained in the myocytes and interstitial tissue (yielding a brown color with a pale blue background) taken from the hearts in the 3W+/40W+ group (Fig 4A). No myocytes were positively stained with the HSP60 antibody in the 3W−/40W−, 3W+/40W− or 3W−/40W+ groups (Fig 4B,C and 4, respectively).

Discussion

There is some clinical evidence that DCM is a late sequel of acute or chronic viral myocarditis[5] Infectious and autoimmune myocarditis has also been extensively proven using murine and rat models[3–5] We previously demonstrated that repetitive CVB3 infection in mice could cause LV dilatation with dysfunction through autoantibodies,

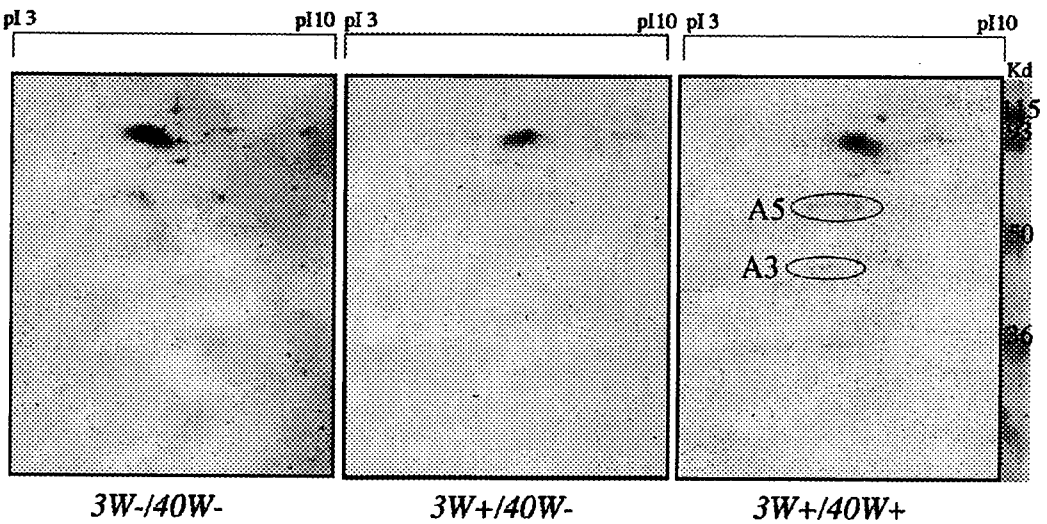

Fig 3. Two-dimensional western blotting with the serum in the 3W−/40W−, 3W+/40W−, and 3W+/40W+ groups. Two spots were detected as A3 and A5 in the membranous fraction that specifically cross-reacted with the serum in the 3W+/40W+ group compared with the other 2 groups. A3 and A5 were recognized as α-cardiac actin and murine HSP60, respectively, by subsequent LC-MS/MS.

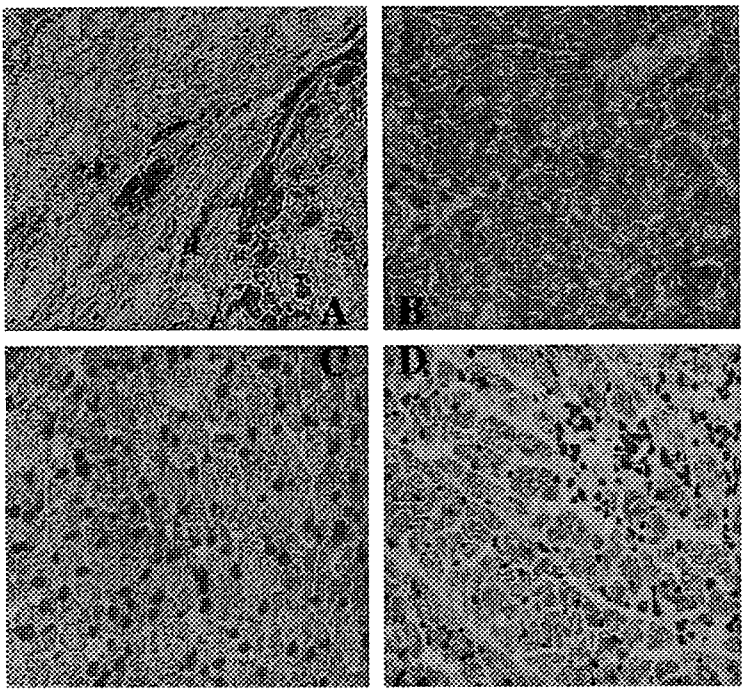

Fig 4. Immunohistochemistry of the myocardium with the anti-HSP60 antibody. The HSP60-positive cells were scattered in the myocardium in the 3W+/40W+ mouse (A). No specific staining for the anti-HSP60 antibody was observed in the heart tissue of either the 3W−/40W− (B), 3W+/40W− (C), or 3W−/40W+ (D) groups.

which were immunologically maximally activated at 2 weeks after the second CVB3 inoculation[5] Moreover, these pathophysiological changes were present even at 8 weeks after the second inoculation. Electron microscopy showed that these antibodies belong to the IgM subtype, and were distributed on the surface of the myocytes and interstitial tissue at 2 weeks after the second viral inoculation in mice. The results of our study are entirely different from the previously reported anti-heart antibodies in viral myocarditis[5] First, in the present study repetitive CVB3 infection produced cardiac dilatation and dysfunction without inflammatory cell infiltration in post-myocarditic mice. This poor T cell response may be related to the protective effect of neutralizing antibody against CVB3 induced by the first inoculation, as well as to CVB3 being less able to cause myocardial lesions related to senescence[6] Second, antibodies that react to the membranous fraction of normal myocytes were produced in the repetitive viral infection, but not in the post-myocarditis mice with simple viral infection. Third, the antibodies were classified as the IgM subtype, as distinct from the other IgG-type antibodies, such as ADP-ATP carrier protein and cardiac sarcoplasmic reticulum calcium ATPase, which were previously identified as cardiac autoantibodies[5] Fourth, the antibodies reacted to the membrane fraction of the myocytes, so that these antibodies identified in the serum of the repetitive myocarditic mice could easily bind the targeting antigen and cause immunological cytotoxicity accompanied by activation of the complementary system in vivo[11] It has also been reported that some anti-heart IgM autoantibodies can activate the complementary system and cause subsequent cardiac damage, especially in membranous proteins such as myolemmal[12] Fifth, we identified 2 autoantibodies (α-cardiac actin and HSP60) against the cardiac membrane protein. Finally, we have already reported that interleukin-1α and tumor necrosis factor-α were elevated in our model[6] They are able to potentiate the immune response and induce cell death, both of which appear to have a special importance in the pathogenesis of myocarditis. As a result, the IgM antibodies, which can activate the complementary system, and cytokines may cooperatively cause the cytotoxic effect on the target myocytes.

In patients with histologically proven myocarditis or familial DCM, autoreactive autoantibodies to components of the myocardium are often present, including intracellular targets such as the ADP/ATP translocator and other mitochondrial proteins[13] Dorffel et al demonstrated that the extraction of autoimmunoreactive antibodies by immunoadsorption results in a functional improvement in hemodynamics in DCM patients[14] Those authors have proven indirectly that autoantibodies against the ADP-ATP carrier[15] contractile proteins of cardiomyocytes, and the cardiac β_1-adrenergic receptor[16,17] contribute to cardiac malfunction in DCM. They proposed that the immunoadsorption may be an additional therapeutic possibility for the acute hemodynamic stabilization of patients with severe DCM. Moreover, Kishimoto et al reported that antibody-mediated immune enhancement is involved in the pathogenesis of CBV3 myocarditis in mice[18] Nishimura et al also proved that PD-1, which binds to the 33-kD protein, may be an important factor contributing to autoimmune cardiomyopathy in mice[19] These results raise the possibility that some form of cardiomyopathy may have a CVB3-induced autoimmune basis, and that identifying possible autoantigen(s) may open up new diagnostic and therapeutic approaches for this disease. Regarding their results, molecular mimicry may be involved in these mechanisms[20] This occurs when an immune response mounted by the host against a specific determinant of an infecting viral or bacterial agent cross-reacts with a similar 'mimicked' host sequence, leading to autoimmunity, and, in some cases, tissue injury and disease. However, one question that has been raised is how these antibodies recognize cytosolic antigen in intact myocytes, because these antigens are isolated and tolerated from circulating antibodies[11] Interestingly, Maish et al demonstrated that anti-membrane antibodies circulated not only in

the peripheral blood, but were also bound to the sarcolemma and interstitial tissue in the endomyocardial biopsy specimens of patients[5] Their results are compatible with our electron microscopy findings, indicating that the antibodies belong to the IgM subtype, and respond to the surface of the myocytes in repetitive CVB3 infection. In this study, we compared the serum of repetitive CVB3 with other groups to identify autoantigens in the myocardium, and identified 2 cardiac antigens in the membranous fraction: α-cardiac actin and HSP60. Although α-cardiac actin is a well-known cytosolic component of myocytes, there is a technical limitation to purifying the membrane fraction in the process of extraction from a heart sample[9] As we observed in our study, α-cardiac actin has already been reported as a cytosolic autoantigen in CVB3 myocarditis[21]

In this study, we demonstrated that HSP60 may be a candidate for a membrane-bound autoantigen in repetitive CVB3 inoculation. The HSP family has been identified as a prominent target of ongoing immune responses during microbial infections. Cross-reactive immune responses between mammalian and microbial HSPs have been suggested as underlying several autoimmune and inflammatory disorders, including chronic arthritis, systemic lupus erythematosus, atherosclerosis, Crohn's disease, and diabetes[22] In addition to constituting an endogenous stress response that protects cells from injury, members of the HSP family are also candidate molecules that potentially signal tissue damage or cellular stress to the immune system, the so-called 'danger theory'. The expression of HSP is upregulated rapidly during several forms of cellular stress, and HSP can be released from damaged tissue[23] Portig et al reported that antibodies against HSP60 were found in the sera of patients with DCM, and may interfere with the functions this stress protein plays in cell physiology (ie, protein transport, protein maturation, and protection of the cell under stress conditions)[24] Latif et al also reported that not only was the anti-heart antibody against HSP60 present in the sera, but HSP60 was upregulated in the myocardium of patients with DCM[10] They confirmed that the cell surface expression of HSP60 after heat stress can be visualized using immunofluorescence. Taken together with our results, these findings suggest that IgM antibodies against α-cardiac actin and HSP60, which were induced by repetitive CVB3 infection, may play an important role in the pathophysiology of the subsequent cardiac dysfunction and dilatation.

Conclusions

In the present study, repetitive CVB3 infection caused cardiac dysfunction and dilatation with an induction of a variety of anti-heart antibodies. Exploring the nature of these autoantibodies found in the sera of our model will provide further immunological and virological insights into the mechanism of subsequent DCM after viral myocarditis.

Acknowledgments

We would like to thank Dr Akira Matsumori (Kyoto University, Kyoto, Japan) for his provision of CVB3. In addition, we would like to thank Rie Ishihara and Kazuko Iwamoto for their excellent technical assistance. This study was supported in part by funds from the Idiopathic Cardiomyopathy Research Group of the Ministry of Health and Welfare of Japan.

References

1. Kriett JM, Kaye MP. The registry of the international society for heart transplantation: Seventh official report, 1990. *J Heart Transplant* 1990; **9:** 323–330.
2. Kawai C. From myocarditis to cardiomyopathy: Mechanisms of inflammation and cell death: Learning from the past for the future. *Circulation* 1999; **99:** 1091–1100.
3. Nakamura H, Yamamura T, Umemoto S, Fukuta S, Shioi T, Matsumori A, et al. Autoimmune response in chronic ongoing myocarditis demonstrated by heterotopic cardiac transplantation in mice. *Circulation* 1996; **94:** 3348–3354.
4. Nakamura H, Kato T, Yamamura T, Yamamoto T, Umemoto S, Sekine T, et al. Characterization of T cell receptor b chains of accumulating T cells in chronic ongoing myocarditis demonstrated by heterotopic cardiac transplantation in mice. *Jpn Circ J* 2001; **65:** 106–110.
5. Maisch B, Ristic AD. Humoral immune response in viral myocarditis. *In*: Cooper LT, editor. Myocarditis: From bench to bedside. New Jersey: Humana Press; 2002; 77–108.
6. Nakamura H, Yamamoto T, Yamamura T, Nakao F, Umemoto S, Shintaku T, et al. Repetitive coxsackievirus infection induces cardiac dilatation in post-myocarditic mice. *Jpn Circ J* 1999; **63:** 794–802.
7. Matsumori A, Kawai C. An experimental model for congestive heart failure after encephalomyocarditis virus myocarditis in mice. *Circulation* 1982; **65:** 1230–1235.
8. Yamaguchi K, Takahashi S, Sasaki K, Tonosaki A. Early expression of intercellular adhesion molecule-1 in the corneal endothelium stimulated by endotoxin: An immuno-scanning electron microscopical study. *Jpn J Ophthalmol* 1996; **40:** 12–17.
9. Kawamura S, Yoshida K, Miura T, Mizukami Y, Matsuzaki M. Ischemic preconditioning translocates PKC-δ and -ε, which mediate functional protection in isolated rat heart. *Am J Physiol* 1998; **275:** 2266–2271.
10. Latif N, Taylor PM, Khan MA, Yacoub MH, Dunn MJ. The expression of heat shock protein 60 in patients with dilated cardiomyopathy. *Basic Res Cardiol* 1999; **94:** 112–119.
11. Wraith DC. Immunological tolerance. *In*: Roitt I, Brostoff J, Male D, editors. Immunology, 5th edn. London: Mosby; 1996; 187–198.
12. Olson TM, Kishimoto Y, Whitby FG, Michels VV. Mutations that alter the surface charge of alpha-tropomyosin are associated with dilated cardiomyopathy. *J Mol Cell Cardiol* 2001; **33:** 723–732.
13. Liu PP, Mason JW. Advances in the understanding of myocarditis. *Circulation* 2001; **104:** 1076–1082.
14. Dorffel WV, Felix SB, Wallukat G, Brehme S, Bestrvater K, Hofmann T, et al. Short-term hemodynamic effects of immunoadsorption in dilated cardiomyopathy. *Circulation* 1997; **95:** 1994–1997.
15. Schulze K, Becker BF, Schauer R, Schultheiss HP. Antibodies to ADP-ATP carrier, an autoantigen in myocarditis and dilated cardiomyopathy, impair cardiac function. *Circulation* 1990; **81:** 959–969.
16. Magnusson Y, Marullo S, Hoyer S, Waagstein F, Andersson B, Vahlne A, et al. Mapping of a functional autoimmune epitope on the β_1-adrenergic receptor in patients with idiopathic dilated cardiomyopathy. *J Clin Invest* 1990; **86:** 1658–1663.
17. Baba A, Yoshikawa T, Chino M. Characterization of anti-myocardial autoantibodies in Japanese patients with dilated cardiomyopathy. *Jpn Circ J* 2001; **65:** 867–873.
18. Kishimoto C, Kurokawa M, Ochiai H. Antibody-mediated immune enhancement in coxsackievirus B3 myocarditis. *J Mol Cell Cardiol* 2002; **34:** 1227–1238.
19. Okazaki T, Tanaka Y, Nishio R, Mitsuiye T, Mizoguchi A, Wang J, et al. Autoantibodies against cardiac troponin I are responsible for dilated cardiomyopathy in PD-1-deficient mice. *Nat Med* 2003; **9:** 1477–1483.
20. Richardson P, McKenna W, Bristow M, Maisch B, Mautner B, O'Connell J, et al. Report of the 1995 World Health Organization/International Society and Federation of Cardiology Task Force on the definition and classification of cardiomyopathies. *Circulation* 1996; **93:** 841–842.
21. Maisch B, Bauer E, Cirsi M, Kochsiek K. Cytolytic cross-reactive antibodies directed against the cardiac membrane and viral proteins in coxsackievirus B3 and B4 myocarditis: Characterization and pathogenetic relevance. *Circulation* 1993; **87**(Suppl 4): IV-49–IV-65.
22. Oldstone MB. Molecular mimicry and autoimmune disease. *Cell* 1987; **50:** 819–820.
23. Wallin RP, Lundqvvist A, More SH, von Bonin A, Kiessling R, Ljunggren HG. Heat-shock proteins as activators of the innate immune system. *Trends Immunol* 2002; **23:** 130–135.
24. Portig I, Pankuweit S, Maish B. Antibodies against stress protein in sera of patients with dilated cardiomyopathy. *J Mol Cell Cardiol* 1997; **29:** 2245–2251.

Safety and Efficacy of Repeated Sauna Bathing in Patients With Chronic Systolic Heart Failure: A Preliminary Report

HIROMITSU MIYAMOTO, MD,[1] HISASHI KAI, MD, PhD,[1,2] HIROYUKI NAKAURA, MD, PhD,[1] KATSUNORI OSADA, MD,[1] YOSHIHIKO MIZUTA, MD,[1] AKIRA MATSUMOTO, MD, PhD,[1] AND TSUTOMU IMAIZUMI, MD, PhD[1,2]

Kurume, Japan

ABSTRACT

Background: We sought to determine the safety and efficacy of repeated 60°C sauna bathing in patients with chronic systolic congestive heart failure (CHF).

Methods and Results: This study included 15 hospitalized CHF patients (New York Heart Association class = 2.8 ± 0.4) in stable clinical condition on conventional treatments. Sauna bathing was performed once per day for 4 weeks. Repeated sauna bathing was safely completed without any adverse effects in all patients. Symptoms improved in 13 of 15 patients after 4 weeks. Sauna bathing decreased systolic blood pressure without affecting heart rate, resulting in significant decrease in the rate-pressure product (6811 ± 1323 to 6292 ± 1093). Echocardiographic left ventricular ejection fraction was significantly increased from 30 ± 11 to 34 ± 11%. Sauna bathing significantly improved exercise tolerance manifested by prolonged 6-minute walking distance (388 ± 110 to 448 ± 118 m), increased peak respiratory oxygen uptake (13.3 ± 1.8 to 16.3 ± 2.1 mL/kg/min), and enhanced anaerobic threshold (9.4 ± 1.2 to 11.5 ± 1.9 mL/kg/min). Four-week bathing significantly reduced plasma epinephrine (40 ± 42 to 21 ± 23 pg/mL) and norepinephrine (633 ± 285 to 443 ± 292 pg/mL). Sauna bathing reduced the number of hospital admission for CHF (2.5 ± 1.3 to 0.6 ± 0.8 per year).

Conclusion: Repeated 60°C sauna bathing was safe and improved symptoms and exercise tolerance in chronic CHF patients. Sauna bathing may be an effective adjunctive therapy for chronic systolic CHF.

Key Words: Thermal therapy, exercise tolerance, echocardiography, catecholamines.

The primary therapeutic goals of chronic congestive heart failure (CHF) are improvement of prognosis and maintenance of quality of life. In this regard, great progress has been achieved by recent advances in pharmacologic treatment using angiotensin-converting enzyme inhibitors,[1,2] angiotensin II receptor blockers,[3,4] β-blockers,[5,6] and aldosterone antagonists.[7] However, many patients on conventional treatment still have impaired quality of life. Therefore, some other modalities of treatment are desirable.

Cardiovascular responses to ordinary hot (80°C) sauna include tachycardia, systolic hypertension, and increased cardiac workload, which are mediated by peripheral vasodilatation and stimulation of the sympathetic nerve system.[8–10] These changes are similar to the response to heat stress. Thus hot sauna bathing is considered to be inappropriate or harmful for CHF patients. However, Tei et al[11] have demonstrated that a single 60°C dry sauna bathing for 15 minutes was tolerable to CHF patients and produced beneficial acute hemodynamic effects, such as increase in cardiac output and decreases in systemic vascular resistance and pulmonary capillary wedge pressure via thermal peripheral vasodilatation. In addition, the same group showed that repeated 60°C sauna bathing for 2 weeks improved subjective well-being and the forearm endothelial function in CHF patients.[12] However, there were no reports on the effects of repeated sauna bathing on the exercise tolerance. Accordingly, the safety and efficacy of repeated 60°C sauna bathing for 4 weeks were investigated in patients with systolic chronic CHF on conventional treatment. For these purposes, we determined the effects of sauna bathing on clinical symptoms, exercise tolerance, neurohumoral factors, and echocardiographic left ventricular ejection fraction (LVEF).

From [1]The Third Department of Internal Medicine and [2]Cardiovascular Research Institute, Kurume University School of Medicine, Kurume, Japan

Manuscript received October 21, 2004; revised manuscript received March 10, 2005; revised manuscript accepted March 11, 2005.

Reprint requests: Hisashi Kai, MD, PhD, The Third Department of Internal Medicine and Cardiovascular Research Institute, Kurume University School of Medicine, 67 Asahimachi, Kurume 830-0011, Japan.

Partially supported and by a Grant-in-Aid for Scientific Research and by a grant for Academic Frontier Project from the Ministry of Education, Science, Sports, Culture, and Technology, Japan.

1071-9164/$ - see front matter

© *2005 Elsevier Inc. All rights reserved.*

doi:10.1016/j.cardfail.2005.03.004

Methods

This study included 15 (12 men and 3 women) patients with chronic CHF (Table 1); 6 with idiopathic dilated cardiomyopathy, 1 with dilated phase of hypertrophic cardiomyopathy, 7 with old myocardial infarction, and 1 with valvular heart disease. Age of the patients ranged from 34 to 75 (mean 62 ± 15) years. Of these patients, 3 and 12 were in New York Heart Association (NYHA) functional class II and III, respectively. This study excluded patients with (1) acute myocardial infarction or unstable angina; (2) uncontrollable tachycardic or bradycardic arrhythmia; (3) acute pulmonary edema; (4) cardiogenic shock; (5) uncontrollable hypertension; (6) systemic disorders such as severe hepatic, renal, hematologic, and malignant diseases; (7) diabetes mellitus under insufficient control; (8) active inflammation (serum C-reactive protein >2.0 mg/mL); (9) anemia (hemoglobin concentration <8.0 mg/mL); or (10) hypoxia (arterial oxygen saturation <70 %).

All patients were in stable clinical condition before this study in our hospital on maintenance doses of conventional medications for chronic CHF, including renin-angiotensin system inhibitor (angiotensin-converting enzyme inhibitors or angiotensin II receptor blockers), β-blocker, diuretics, and digitalis.[13] Of the 15 patients, all had a renin-angiotensin system inhibitor and furosemide, 9 had spironolactone, and 11 had digitalis (Table 1). Although 5 patients had a β-blocker, β-blockers were not used in the remaining 10 patients because of intolerable bradycardia or hypotension. Their medications were not changed during the study. This study complied with the Declaration of Helsinki. The study protocol was approved by the Ethics Committee of Kurume University, and written informed consent was obtained from each patient before participation.

Sauna Bathing

A far infrared-ray sauna system (Olympia Co, Miyazaki, Japan) was used. Patients were placed in the sitting position in a 60°C dry sauna for 15–20 minutes, and then rested on a reclining chair with sufficient warmth provided by blankets in a temperature-controlled room at 25°C for 30 minutes.[11] Patients were weighed before and after sauna bathing, and oral hydration with water (100–200 mL) was supplied to compensate for water loss.

Study Protocol

Patients underwent 60°C sauna bathing once per day, 5 days per week, for 4 weeks. Exercise tolerance, plasma levels of neurohumoral factors, echocardiogram, and chest roentgenogram were evaluated just before and immediately after 4-week bathing. Fasting blood samples were drawn from the antecubital vein early in the morning. Plasma epinephrine, norepinephrine and brain natriuretic peptide (BNP) were measured at a commercial available laboratory (SRL, Fukuoka, Japan). The left ventricular (LV) and left atrial dimensions were measured on the M-mode echocardiograms, and LVEF was calculated by the modified Simpson's method.[14]

Assessment of Clinical Symptoms

Clinical symptoms (shortness of breath, fatigue, appetite loss, insomnia, and constipation) were evaluated by a self-assessment quality-of-life questionnaire.[12] After 4 weeks of sauna bathing, questionnaire sheets were given to patients and they were asked to choose 1 from 4 grades: "remarkably improved," "improved," "no change," or "worsened," as compared with the baseline, for each symptom. Based on the results, patients were categorized to the following 3 groups: improved patients with "remarkable improvement" or "improvement" of more than 2 items, worsened patients with "worsening" of at least more than 1 item, and the others.

Exercise Tolerance Tests

In all patients, a 6-minute walk testing was carried out and the total walking distance was determined. For further quantitative evaluation for exercise tolerance, in the last 5 consecutive patients (Patients 11–15), cardiopulmonary exercise testing was performed

Table 1. Patient Profile

Patient Number	Age (y)	Gender	Diagnosis	NYHA Class	Diabetes Mellitus	HC	Medication				
							ACEI or ARB	β-Blocker	Furosemide	Spironolacton	Digitalis
1	61	Male	DCM	III	−	−	+	−	+	−	+
2	63	Female	dHCM	III	+	−	+	−	+	−	+
3	34	Male	DCM	III	+	−	+	+	+	+	+
4	53	Male	OMI	III	+	+	+	−	+	+	+
5	38	Male	DCM	III	−	−	+	−	+	+	+
6	74	Male	OMI	III	−	−	+	−	+	+	+
7	74	Female	DCM	III	−	−	+	+	+	−	+
8	70	Female	OMI	III	+	+	+	−	+	+	+
9	47	Male	OMI	II	−	+	+	+	+	+	+
10	71	Male	VHD	II	−	−	+	−	+	−	+
11	68	Male	OMI	III	+	+	+	−	+	+	−
12	77	Male	OMI	III	+	−	+	−	+	+	+
13	72	Male	DCM	III	−	−	+	−	+	−	−
14	62	Male	OMI	II	+	+	+	+	+	+	−
15	75	Male	DCM	III	−	−	+	+	+	−	−

DCM, dilated cardiomyopathy; dHCM, dilated phase of hypertrophic cardiomyopathy; OMI, old myocardial infarction; VHD, valvular heart disease; ACEI: angiotensin-converting enzyme inhibitor; ARB, angiotensin II receptor blocker.

Diabetes mellitus was defined as hemoglobin A1c greater than 5.8%.

Hypercholesterolemia (HC) was defined as total cholesterol greater than 220 mg/mL.

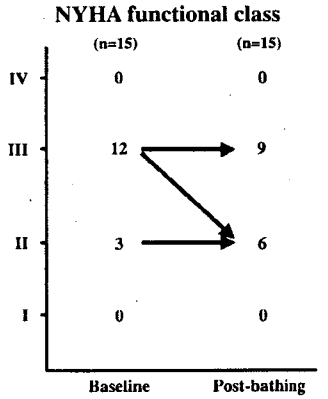

Fig. 1. Changes in New York Heart Association (NYHA) functional class.

using a bicycle ergometer. The peak respiratory oxygen uptake (peak $\dot{V}O_2$) was calculated, and the anaerobic threshold was determined by the V-slope method. The patient profile of the subgroup was similar to that of the whole patients studied.

To confirm that the patients were in stable condition and to evaluate the consistency of repeated measurements of exercise tolerance, 6-minute walking test and cardiopulmonary exercise testing were repeated 1–2 weeks and just before the entry of the study protocol.

Statistical Analysis

Values are mean ± SD. Paired- and unpaired *t*-tests were performed for comparisons between the baseline and postbathing and between 2 groups, respectively. For exercise tolerance tests, Kruskal-Wallis test was used. A value of $P < .05$ was considered statistically significant.

Results

All patients enrolled in this study completed 4-week repeated sauna bathing without any adverse symptoms and events. Of 12 patients with NYHA functional class III, 3 improved to functional class II (Fig. 1). As shown in Table 2, the self-assessment quality-of-life questionnaire revealed that 13 of 15 patients were categorized as the improved group. Improvements of shortness of breath and fatigue were most evident. Body weight did not change (Table 3). Repeated sauna bathing decreased systemic blood pressure without changes in heart rate, resulting in significant decrease in the rate-pressure product. And LVEF improved from 30 ± 11 to 34 ± 11%. Cardiothoracic ratio was slightly, yet significantly, decreased.

Exercise Tolerance

As shown in Fig. 2, the patients were stable before sauna bathing. Just before sauna bathing, 6-minute walking distance was 388 ± 110 m. Four-week sauna bathing improved 6-minute walking distance in each patient, and the average was significantly increased to 448 ± 118 m. Baseline examination revealed markedly reduced peak $\dot{V}O_2$ and anaerobic threshold (13.3 ± 1.8 and 9.4 ± 1.2 mL/kg/min, respectively). In each patient, repeated sauna bathing improved peak VO_2 and anaerobic threshold, and the averages were significantly increased to 16.3 ± 2.1 and 11.5 ± 1.9 mL/kg/min, respectively.

Neurohumoral Factors

At baseline, plasma catecholamines and BNP were elevated (Table 3). Repeated sauna bathing markedly reduced plasma epinephrine and norepinephrine levels. Although sauna bathing tended to decrease plasma BNP levels, the effects were inconsistent and the changes did not reach the statistical significance.

Hospital Admission for CHF

During the 12-month follow-up, 2 of 15 patients died of CHF. In the remaining 13 patients, the number of hospital admission for CHF during 1 year was compared before

Table 2. Changes of Symptoms

Patient Number	Self-Assessment Quality-of-Life Questionaere						New York Heart Association Functional Class	
	Shortness of Breath	Fatigue	Appetite Loss	Insomnia	Constipation	Overall Assessment	Baseline	Posttreatment
1	1 +	1 +	0	1 +	1 +	Improved	III	III
2	1 +	1 +	0	1 +	1 +	Improved	III	III
3	0	0	0	0	1 +	Unchanged	III	III
4	1 +	2 +	1 +	0	1 +	Improved	III	III
5	1 +	1 +	0	0	0	Improved	III	III
6	1 +	1 +	1 +	2 +	1 +	Improved	III	III
7	1 +	1 +	1 +	0	1 +	Improved	III	III
8	1 +	1 +	1 +	0	1 +	Improved	III	III
9	1 +	1 +	0	0	0	Improved	II	II
10	1 +	1 +	0	0	1 +	Improved	II	II
11	1 +	1 +	1 +	1 +	0	Improved	III	II
12	2 +	0	0	2 +	0	Improved	III	II
13	1 +	1 +	0	0	1 +	Improved	III	II
14	0	1 +	0	0	0	Unchanged	II	II
15	2 +	2 +	1 +	1 +	0	Improved	III	III

2 +, remarkably improved; 1 +, improved; 0, unchanged; 1 −, worsened.

Table 3. Effects of 4-Week Sauna Treatment

	Baseline	Postbathing	
Body weight (kg)	60 ± 11	60 ± 11	NS
Systolic blood pressure (mm Hg)	101 ± 13	98 ± 14	$P < .05$
Heart rate (/min)	73 ± 12	72 ± 12	NS
Rate-pressure product	6811 ± 1323	6292 ± 1093	$P < .01$
Echocardiographic findings			
Left atrial dimension (mm)	48 ± 12	46 ± 12	NS
Left ventricular end-diastolic dimension (mm)	68 ± 7	68 ± 9	NS
Left ventricular ejection fraction (%)	30 ± 11	34 ± 11	$P < .05$
Chest roentogenographic finding			
Cardiothoracic ratio (%)	59 ± 7	58 ± 7	$P < .05$
Neurohumoral factors			
Epinephrine (pg/mL)	40 ± 42	21 ± 23	$P < .05$
Norepinephrine (pg/mL)	633 ± 285	443 ± 292	$P < .01$
Brain natriuretic peptide (pg/mL)	456 ± 469	399 ± 393	NS

and after sauna bathing (Fig. 3). In each patient, sauna bathing decreased the number of admission for CHR.

Discussion

The present study demonstrated for the first time that repeated 60°C sauna bathing for 4 weeks improved exercise tolerance and clinical symptoms in patients with chronic systolic CHF on conventional treatments. Moreover, LVEF was improved, and elevated plasma epinephrine and norepinephrine were decreased. No apparent adverse events were experienced. During the follow-up, sauna bathing reduced the number of hospital admission for CHF.

Most of patients were subjectively in NYHA functional class III (mean NYHA class = 2.8 ± 0.4). At baseline, plasma BNP and norepinephrine were greater than 450 pg/mL and 600 pg/mL, respectively, indicating that the patients were in NYHA class more than III.[19] Echocardiography revealed LV dilation with LV end-diastolic dimension of 68 mm in association with reduced LVEF of 30%, indicating remarkably impaired LV function. Moreover, average 6-minute walking distance was less than 400 m, associated with low peak $\dot{V}O_2$ <14 mL/kg/min. Thus the enrolled patients were subjectively or objectively in severe CHF. Nonetheless, sauna bathing was safely performed. Conventional hot (80°C) sauna bathing is contraindicated for severe CHF patients because thermal stress increases cardiac workload and sympathetic activity.[12–14] The present study suggests that repeated 60°C sauna bathing can be safely performed even in chronic systolic CHF patients.

The symptoms were improved in 13 of 15 patients, and no patients experienced worsening of symptoms (Table 2). Therefore, repeated sauna bathing was effective for improvement of subjective well-being in chronic CHF patients on conventional treatments. However, because only 3 patients had improvement in NYHA functional class, the subjective improvement may have been placebo effects. Thus we evaluated exercise tolerance such as 6-minute walking distance and peak $\dot{V}O_2$, which are better and more objective indices of improvement. They all had prolongation of 6-minute walking distance, and 5 had improved cardiopulmonary exercise tolerance. Although we did not have the control group, patients had the stable exercise tolerance before sauna bathing (Fig. 2), indicating that the effects were not "warm-up" effects. Thus sauna bathing was effective for improvements of symptoms and exercise tolerance.

Several mechanisms whereby repeated sauna bathing improved exercise tolerance are considered. The most likely one was improvement of cardiac performance; LVEF was improved from 30% to 34% and the cardiac silhouette got

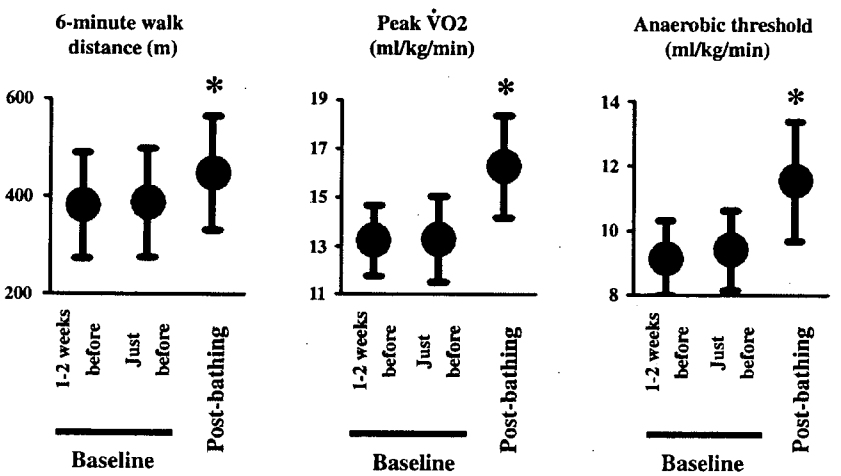

Fig. 2. Four-week repeated sauna bathing improved 6-minute walking distance in all patients (left, bar = 1 × SD [n = 15]). In a subgroup (Patients 11–15), the peak $\dot{V}O_2$ (middle) and anaerobic threshold (right) were improved after 4 weeks in each patient (bar = 1 × SD [n = 5]). At baseline, exercise tolerance tests were repeated 1–2 weeks and just before sauna bathing. *$P < .05$ versus just before sauna bathing.

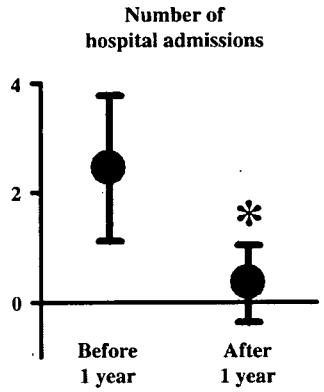

Fig. 3. Number of hospital admission for chronic heart failure in the 12-month period before (before) and after sauna bathing (after). Bar = 1 × SD (n = 13). $^*P < .01$ versus before.

smaller. The increased cardiac function was not due to decrease in preload (water loss), because the body weight did not differ before and after repeated bathing. Although we did not examine it in this study, reduction in afterload (peripheral vascular resistance) could have been responsible because blood pressure decreased (Table 3) and because Tei et al have shown that acute sauna bathing greatly decreases peripheral vascular resistance,[15] and that 2-week sauna bathing improves endothelial function.[16] The decreased plasma catecholamine levels indicate attenuated sympathetic nerve activity by sauna bathing. Although we were not able to determine whether the attenuated sympathetic nerve activity was directly caused by sauna bathing or because of improvement of heart failure, decreased sympathetic nerve activity is a good prognostic sign. It remains unclear why BNP levels did not decrease despite clinical improvement.

In the present study, 4-week sauna bathing reduced the number of hospital admission for CHF. Although the number of patients studied was too small, the observation may raise the possibility that the beneficial effects remain longer even after the cessation of sauna bathing. The mechanisms of the long lasting effects are unknown.

The small number of patients studied limits our interpretations and discussion in this study. Assessment of long-term survival rate was not an objective of the study. Another important limitation is the lack of the control group who did not receive sauna bathing, because blinded study was not feasible. Instead, we had an internal control as described previously.

Conclusions

Repeated 60°C sauna bathing for 4 weeks improved not only well-being but also exercise tolerance in chronic systolic CHF patients on conventional treatments. It is suggested that repeated sauna bathing is a safe and effective adjunctive therapy for chronic CHF.

References

1. The SOLVD Investigators. Effect of enalapril on survival in patients with reduced left ventricular ejection fractions and congestive heart failure. N Engl J Med 1991;325:293–302.
2. The SOLVD Investigators. Effect of enalapril on mortality and the development of heart failure in asymptomatic patients with reduced left ventricular ejection fractions. N Engl J Med 1992;327:685–91.
3. Cohn JN, Tognoni G. Valsartan Heart Failure Trial Investigators. A randomized trial of the angiotensin-receptor blocker valsartan in chronic heart failure. N Engl J Med 2001;345:1667–75.
4. Pfeffer MA, Swedberg K, Granger CB, Held P, McMurray JJ, Michelson EL, et al. Effects of candesartan on mortality and morbidity in patients with chronic heart failure: the CHARM-Overall programme. Lancet 2003;362:759–66.
5. Packer M, Bristow MR, Cohn JN, Colucci WS, Fowler MB, Gilbert EM, et al. The effect of carvedilol on morbidity and mortality in patients with chronic heart failure. N Engl J Med 1996;334:1349–55.
6. Packer M, Coats AJ, Fowler MB, Katus HA, Krum H, Mohacsi P, et al. Effects of carvedilol on survival in severe chronic heart failure. N Eng J Med 2001;344:1651–8.
7. Pitt B, Zannad F, Remme WJ, Cody R, Castaigne A, Perez A, et al. The effect of spironolactone on morbidity and mortality in patients with severe heart failure. N Engl J Med 1999;341:709–17.
8. Shoenfeld Y, Sohar E, Ohry A, Shapiro Y. Heat stress: comparison of short exposure to severe dry and wet heat in saunas. Arch Phys Med Rehabil 1976;57:126–9.
9. Vuori I. Sauna bather's circulation. Ann Clin Res 1988;20:249–56.
10. Eisalo A, Luurila OJ. The Finnish sauna and cardiovascular diseases. Ann Clin Res 1988;20:267–70.
11. Tei C, Horikiri Y, Park JC, Jeong JW, Chang KS, Toyama Y, et al. Acute hemodynamic improvement by thermal vasodilation in congestive heart failure. Circulation 1995;91:2582–90.
12. Kihara T, Biro S, Imamura M, Yoshifuku S, Takasaki K, Ikeda Y, et al. Repeated sauna treatment improves vascular endothelial and cardiac function in patients with chronic heart failure. J Am Coll Cardiol 2002;39:754–9.
13. Hunt SA, Baker DW, Chin MH, Cinquegrani MP, Feldman AM, Francis GS, et al. ACC/AHA Guidelines for the evaluation and management of chronic heart failure in the adult: executive summary. A report of the American College of Cardiology/American Heart Association Task Force on practice guidelines (Committee to revise the 1995 guidelines for the evaluation and management of heart failure). Circulation 2001;104:2996–3007.
14. Schiller NB, Acquatella H, Ports TA, Drew D, Goerke J, Ringertz H, et al. Left ventricular volume from paired biplane two-dimensional echocardiography. Circulation 1979;60:547–55.
15. Latini R, Masson S, Anand I, Judd D, Maggioni AP, Chiang YT, et al. Valsartan Heart Failure Trial Investigators. Effects of valsartan on circulating brain natriuretic peptide and norepinephrine in symptomatic chronic heart failure: the Valsartan Heart Failure Trial (Val-HeFT). Circulation 2002;106:2454–8.
16. Latini R, Masson S, Anand I, Salio M, Hester A, Judd D, et al. For the Val-HeFT Investigators. The comparative prognostic value of plasma neurohormones at baseline in patients with heart failure enrolled in Val-HeFT. Eur Heart J 2004;25:292–9.

ELSEVIER

Cardiovascular Research 73 (2007) 794–805

Cardiovascular Research

www.elsevier.com/locate/cardiores

Soluble TNF receptors prevent apoptosis in infiltrating cells and promote ventricular rupture and remodeling after myocardial infarction

Yoshiya Monden [a], Toru Kubota [a,*], Takaki Tsutsumi [a], Takahiro Inoue [a], Shunichi Kawano [a], Natsumi Kawamura [a], Tomomi Ide [a], Kensuke Egashira [a], Hiroyuki Tsutsui [b], Kenji Sunagawa [a]

[a] *Department of Cardiovascular Medicine, Kyushu University Graduate School of Medical Sciences, 3-1-1 Maidashi, Higashi-ku, Fukuoka 812-8582, Japan*
[b] *Department of Cardiovascular Medicine, Hokkaido University Graduate School of Medicine, Kita-15, Nishi-7, Kita-ku, Sapporo 060-8638, Japan*

Received 7 September 2006; received in revised form 30 November 2006; accepted 19 December 2006
Available online 23 December 2006
Time for primary review 27 days

Abstract

Objective: Tumor necrosis factor (TNF)-α induced in damaged myocardium has been considered to be cardiotoxic. However, the negative results of RENEWAL and ATTACH prompt us to reconsider the role of TNF-α in cardiovascular diseases. The present study aimed to evaluate the effects of soluble TNF receptor treatment on myocardial infarction (MI).
Methods: An adenovirus encoding a 55-kDa TNF receptor-IgG fusion protein (AdTNFR1) was used to neutralize TNF-α, and an adenovirus encoding LacZ (AdLacZ) served as control. In the pre-MI treatment protocol, mice were given an intravenous injection of AdTNFR1 or AdLacZ 1 week before left coronary artery ligation to induce MI. In the post-MI treatment protocol, mice were treated with AdTNFR1 or AdLacZ 1 week after left coronary ligation.
Results: Treatment with AdTNFR1 neutralized bioactivity of TNF-α that was activated after MI and prevented apoptosis of infiltrating cells in infarct myocardium. However, pre-MI treatment with AdTNFR1 promoted ventricular rupture by reducing fibrosis with further activation of matrix metalloproteinase (MMP)-9. Post-MI treatment with AdTNFR1 exacerbated ventricular dysfunction and remodeling, with enhanced fibrosis of non-infarct myocardium with further MMP-2 activation.
Conclusions: Both pre- and post-MI treatments with AdTNFR1 were deleterious in a mouse MI model. Thus, TNF-α may play not only toxic but also protective roles in MI.
© 2006 European Society of Cardiology. Published by Elsevier B.V. All rights reserved.

Keywords: Apoptosis; Cytokines; Infarction; Matrix metalloproteinases; Remodeling

1. Introduction

Tumor necrosis factor-α (TNF-α) is a proinflammatory cytokine that exerts a wide range of biological activities [1]. TNF-α is induced in the failing human heart [2], and considered to be cardiotoxic, because in vitro studies have shown that TNF-α suppresses cardiac contractility [3], provokes myocardial hypertrophy [4] and induces apoptosis in cardiac myocytes [5]. It also has direct effects on the matrix and collagen framework, and is a potential major contributor to cardiac remodeling [6,7]. However, in anti-cytokine clinical trials, the use of either a soluble TNF receptor (RENEWAL) [8] or an anti-TNF antibody (ATTACH) [9] was not beneficial to patients with heart failure. Especially, patients who received the high dose (10 mg/kg) of infliximab (anti-TNF antibody) were more likely to die or be hospitalized for heart failure than patients in the placebo group. High doses of anti-TNF antibodies might have exacerbated the clinical condition of patients with moderate-to-severe chronic heart failure. These results suggest that TNF-α may not be exclusively toxic but may be partially protective in cardiovascular diseases.

Accumulated evidence indicates that cytokines are important mediators of wound healing and remodeling after myocardial infarction (MI). However, the roles of these

* Corresponding author. Tel.: +81 92 642 5359; fax: +81 92 642 5374.
E-mail address: kubotat@cardiol.med.kyushu-u.ac.jp (T. Kubota).

0008-6363/$ - see front matter © 2006 European Society of Cardiology. Published by Elsevier B.V. All rights reserved.
doi:10.1016/j.cardiores.2006.12.016

cytokines in MI remain controversial. Blockade of these cytokines has been reported to be beneficial [10–13], deleterious [14,15], or bidirectional [16,17]. Therefore, the present study was designed to assess the role of TNF-α induction in the process of wound healing and cardiac remodeling after MI. We used soluble TNF receptors to block the bioactivity of TNF-α [18]. Our results indicated that treatment with soluble TNF receptors prevented apoptosis, but significantly promoted ventricular rupture and remodeling with further activation of matrix metalloproteinases (MMPs) after MI. These results support the hypothesis that TNF-α may play not only toxic but also protective roles in MI.

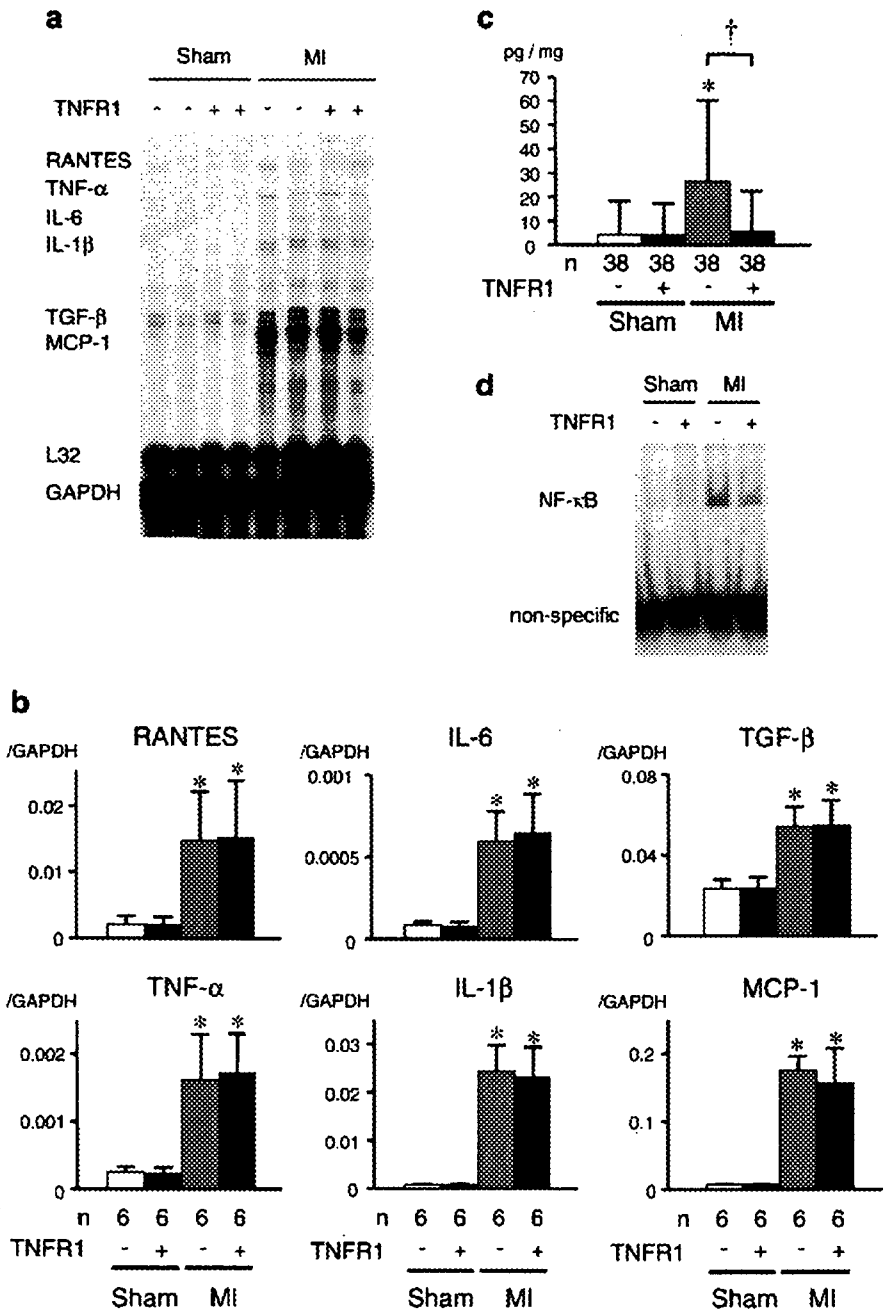

Fig. 1. Multi-probe RNase protection assay for proinflammatory cytokines and chemokines in infarct myocardium on day 3 after MI: a representative assay (a) and summarized data of densitometric analysis (b). Each value is normalized to that of GAPDH in each template set as an internal control. Cytotoxicity assay for TNF-α in infarct myocardium using WEHI cell line (c). Electrophoretic mobility shift assay for activation of NF-κB in infarct myocardium (d). Values are mean±SD. TNFR1 (−) indicates pre-MI treatment with AdLacZ; TNFR1 (+), pre-MI treatment with AdTNFR1; Sham, sham-operated mice; MI, coronary ligated mice. *$p<0.05$ vs. Sham/LacZ mice, †$p<0.05$ vs. MI/LacZ mice.

2. Methods

2.1. Animal model

An MI model was produced in male ICR mice (8–10 weeks old, weighing 35–40 g) by ligating the left coronary artery [10,16,19]. Sham operation without coronary artery ligation was also performed. This study was reviewed by the Committee of the Ethics on Animal Experiment, Kyushu University Graduate School of Medical Sciences and conducted in compliance with the Guideline for Animal Experiment of Kyushu University and the Japanese Law (No.105) and Notification (No. 6). The investigation conforms to the *Guide for the Care and Use of Laboratory Animals* published by the US National Institutes of Health (NIH Publication No. 85-23, revised 1996).

2.2. Experimental design

To block the activity of TNF-α, 10^9 pfu of replication-deficient recombinant adenovirus was used, which encodes the extracellular domain of the human 55-kDa TNF receptor (soluble TNFR1) coupled with a mouse IgG heavy chain (AdTNFR1), and has been proven to suppress myocardial inflammation secondary to TNF-α overexpression in our previous study [18]. An adenovirus encoding LacZ (AdLacZ) served as control. To determine the effects of soluble TNF receptors on early ventricular rupture and late remodeling after MI, two independent protocols were performed. In the pre-MI treatment protocol, four experimental groups were studied: Sham/LacZ (n=63), Sham/TNFR1 (n=63), MI/LacZ (n=155), and MI/TNFR1 (n=161). AdTNFR1 or AdLacZ was injected intravenously 1 week before left coronary artery ligation, and the effects of TNF-α blockade on early ventricular rupture were examined on days 1, 3 and 14 after MI. In the post-MI treatment protocol, four experimental groups were studied: Sham/LacZ (n=19), Sham/TNFR1 (n=18), MI/LacZ (n=36), and MI/TNFR1 (n=38). AdTNFR1 or AdLacZ was injected intravenously 1 week after left coronary artery ligation, and the effects of TNF-α blockade on late remodeling were examined on day 28 after MI. For both protocols, the mice were randomly assigned independently to the four experimental groups. Due to the high mortality in MI groups, the number of MI mice used was 2–3 times greater than the number of Sham mice.

Table 1
Characteristics of animal models (day 3)

	Sham/LacZ (n=16)	Sham/TNFR1 (n=15)	MI/LacZ (n=25)	MI/TNFR1 (n=26)
Echocardiographic data (under anesthesia)				
Heart rate (bpm)	486±26	485±24	490±17	487±13
LV EDD (mm)	3.4±0.1	3.3±0.2	3.8±0.4*	3.9±0.3*
LV ESD (mm)	2.2±0.1	2.1±0.1	3.1±0.4*	3.2±0.3*
Fractional shortening (%)	34.1±1.9	35.2±1.5	19.2±3.3*	17.6±2.3*
Infarct wall thickness (mm)	–	–	0.63±0.09	0.64±0.08
Non-infarct wall thickness (mm)	0.81±0.04	0.81±0.04	0.82±0.04	0.80±0.03
Hemodynamic data (tail-cuff system, awake)				
Heart rate (bpm)	630±53	623±54	635±86	636±92
Systolic blood pressure (mm Hg)	112±8	113±7	103±11	103±11
Organ weight data				
Body wt (g)	38.0±1.4	37.4±2.0	33.5±2.0*	33.0±2.5*
Lung wt/Body wt (mg/g)	5.17±0.33	5.28±0.24	7.83±2.52*	7.56±1.92*
Pleural effusion (%)	0	0	20.0	19.2
N			12	12
Infarct area (%)	–	–	53.1±4.3	54.7±3.8

LV, left ventricular; EDD, end-diastolic diameter; ESD, end-systolic diameter; wt, weight. Values are mean±SD. *P<0.05 vs. Sham/LacZ.

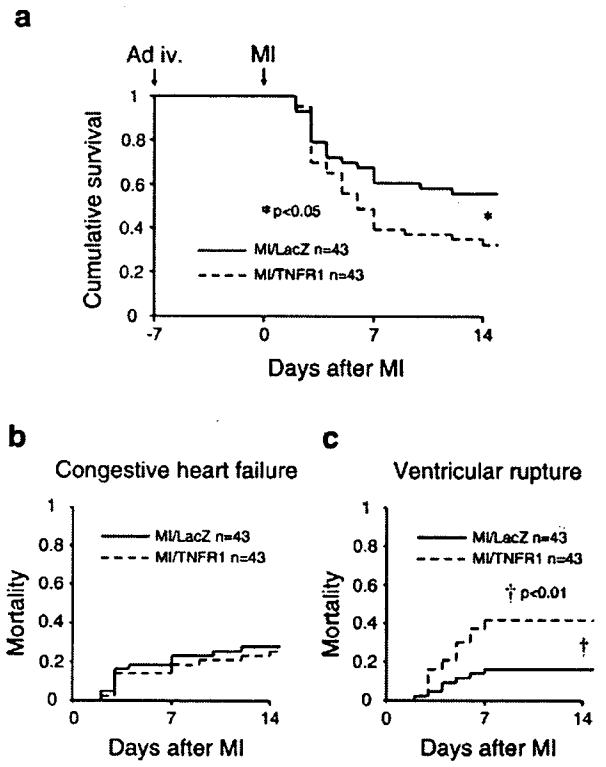

Fig. 2. Kaplan–Meier survival curves of coronary ligated mice with or without pre-MI TNFR1 treatment (a). Mortality of coronary ligated mice from congestive heart failure (b) and ventricular rupture (c). *p<0.05 vs. MI/LacZ mice, †p<0.01 vs. MI/LacZ mice.

2.3. Enzyme-linked immunosorbent assay (ELISA)

Human TNFR1 protein levels were assessed by ELISA (Quantikine, No. DRT100, R&D Systems) [18].

2.4. RNase protection assay (cytokine gene expression)

Multi-probe RNase protection assays (RPA) were performed according to the manufacture's protocol (RiboQuant,

Table 2
Characteristics of animal models (day 14)

	Sham/LacZ (n=9)	Sham/TNFR1 (n=10)	MI/LacZ (n=24)	MI/TNFR1 (n=14)
Echocardiographic data (under anesthesia)				
Heart rate (bpm)	466±15	463±14	459±47	469±55
LV EDD (mm)	3.4±0.3	3.4±0.3	5.5±0.3*	5.5±0.4*
LV ESD (mm)	2.2±0.3	2.3±0.3	4.8±0.3*	4.8±0.4*
Fractional shortening (%)	34.6±2.1	34.4±2.1	12.5±2.1*	13.4±3.0*
Infarct wall thickness (mm)	–	–	0.27±0.05	0.24±0.05
Non-infarct wall thickness (mm)	0.80±0.00	0.79±0.04	0.93±0.08*	0.88±0.08*
Organ weight data				
Body wt (g)	39.5±1.7	38.1±2.5	37.3±3.7	35.7±3.7*
Lung wt/Body wt (mg/g)	5.16±0.32	5.39±0.39	10.31±4.00*	9.89±2.77*
Pleural effusion (%)	0	0	95.5	100
Infarct area (%)	–	–	58.6±2.2	57.5±1.6

LV, left ventricular; EDD, end-diastolic diameter; ESD, end-systolic diameter; wt, weight. Values are mean±SD. *P<0.05 vs. Sham/LacZ.

PharMingen, San Diego, California, USA) using a custom template set containing probes for murine RANTES, TNF-α, IL-6, IL-1β, TGF-β, monocyte chemotactic protein-1(MCP-1), L32, and GAPDH (No. 557310) [10,16,18].

2.5. Determination of tissue TNF-α bioactivity

Myocardial TNF-α bioactivity was measured with a cytotoxicity assay using the TNF-sensitive WEHI murine fibrosarcoma cell line [11].

2.6. Electrophoretic mobility shift assay (EMSA)

Activation of NF-κB was evaluated by the electrophoretic mobility shift assay (EMSA) according to the manufacture's instructions (Gel Shift Assay System E3300, Promega, Madison, Wisconsin, USA) [20]. Nuclear protein was isolated from the myocardium as previously reported [20]. Samples were resolved on a 5% acrylamide gel in 0.25% Tris–borate–EDTA buffer.

2.7. Echocardiographic and hemodynamic measurements

Echocardiographic studies were performed using an ultrasonographic system (ALOKA SSD-5500; Tokyo, Japan) as previously described [10,16,19]. In the pre-MI treatment protocol, arterial blood pressure and heart rate were also measured awake on day 3 with the use of a noninvasive tail–cuff system (BP-98A, Softron). In the post-MI treatment protocol, a 1.4 Fr micromanometer-tipped catheter (Millar) was inserted into the left ventricle (LV) through the right carotid artery to measure LV pressure on day 28 under anesthesia with 2.5% Avertin (14 μl/g body weight, IP, Aldrich Chemical Co) [10,16,19].

2.8. Infarct size and pathological analysis

Infarct size was determined by methods described previously for mice [10,16,19]. Briefly, the LV was cut from apex to base into 4 transverse sections. Infarct length was measured along the endocardial and epicardial surfaces from each of the LV sections, and the values from all specimens were summed. Total LV circumference was calculated as the sum of endocardial and epicardial segment lengths from all LV sections. Infarct size (in percent) was calculated as total infarct circumference divided by total LV circumference. Picrosirius red staining was performed to observe interstitial collagen fibers and determine collagen volume fraction [10,19]. Collagen volume fraction was measured at 6 fields for each heart. Myocardial infiltration was quantified by determining nuclear density (nuclei/mm^2) on hematoxylin and eosin stained sections [18]. Because it is difficult to differentiate inflammatory cells from myocytes and/or fibroblasts, all nuclei were included. In each mouse, six independent high-power fields were analyzed and averaged. To further determine the number of macrophages, an immunohistochemical analysis using a specific antibody against mouse Mac-3 (macrophage marker, BD Pharmingen) was performed.

2.9. Apoptosis

Apoptosis was evaluated by a ligation-mediated PCR fragmentation (DNA laddering) assay (Maxim Biotech Inc) [20]. In addition, LV tissue sections were stained for terminal deoxynucleotidyl transferase-mediated dUTP nick end-labeling (TUNEL) to detect apoptotic cell [20]. The number of TUNEL-positive nuclei was counted, and the data were normalized per total nuclei identified as hematoxylin-positive staining in the same sections.

2.10. MMP zymography

Gelatin zymography was performed as previously described [19]. The zymograms were digitized, and the size-fractionated bands, which indicated the MMP proteolytic levels, were measured as the integrated optical density in a rectangular region of interest.

2.11. Double immunohistochemical staining for MMP-9 and Mac-3

Double immunohistochemical staining for MMP-9 (Santa Cruz Biotech.) and Mac-3 (macrophage marker, BD Pharmingen) in infarct myocardial sections were performed by routine protocols at our laboratory to localize MMP-9 with potential MMP-producing cells [21].

2.12. Statistical analysis

The results are presented as mean±SD. Statistical comparisons were performed using ANOVA with Students–Newman–

Keuls post hoc test or unmatched Student's *t*-test where appropriate. When the Levene test for homogeneity of variance revealed significant differences between groups, nonparametric tests (Kruskal–Wallis, the Mann–Whitney *U* test) were performed on the variables. Survival analysis was performed by the Kaplan–Meier method, and between-group difference in survival was tested by the log-rank test. Differences were considered significant at a p value less than 0.05.

3. Results

3.1. Pre-MI treatment protocol

3.1.1. TNF-α in infarct myocardium

Plasma levels of human TNFR1 10 days after inoculation with AdTNFR1 (or 3 days after MI or sham operation) were 512.7±93.6 (SD) μg/ml, which were similar to our previous report [18]. Multi-probe RPA was used to evaluate expression of proinflammatory cytokines and chemokines in infarct myocardium 3 days after MI or sham operation (Fig. 1a). Transcript levels of TNF-α, IL-1β, IL-6, TGF-β, MCP-1, and RANTES were significantly up-regulated in infarct myocardium, and were not affected by treatment with TNFR1 (Fig. 1b). However, as summarized in Fig. 1c, cytotoxic activity of TNF-α, which was significantly increased in infarct myocardium, was significantly attenuated by treatment with TNFR1. To examine the downstream signals of TNF-α, activation of NF-κB was evaluated in infarct myocardium on day 3 using EMSA. As shown in Fig. 1d, increased activation of NF-κB in infarct myocardium was attenuated by TNFR1 treatment ($n=4$ per group).

3.1.2. Increased ventricular rupture with TNFR1 treatment

Survival analysis was performed in four groups of mice, including Sham/LacZ, Sham/TNFR1, MI/LacZ, and MI/TNFR1. Mice that died within 12 h after the operation were excluded, because early operative mortality was not different between MI/LacZ (23.2%) and MI/TNFR1 mice (21.8%). No mice died after sham operation. In contrast, as shown in Fig. 2a, 19 of 43 MI/LacZ and 29 of 43 MI/TNFR1 mice died by the end of 2 weeks after coronary ligation. Statistical analysis indicated that pre-MI treatment with soluble TNF

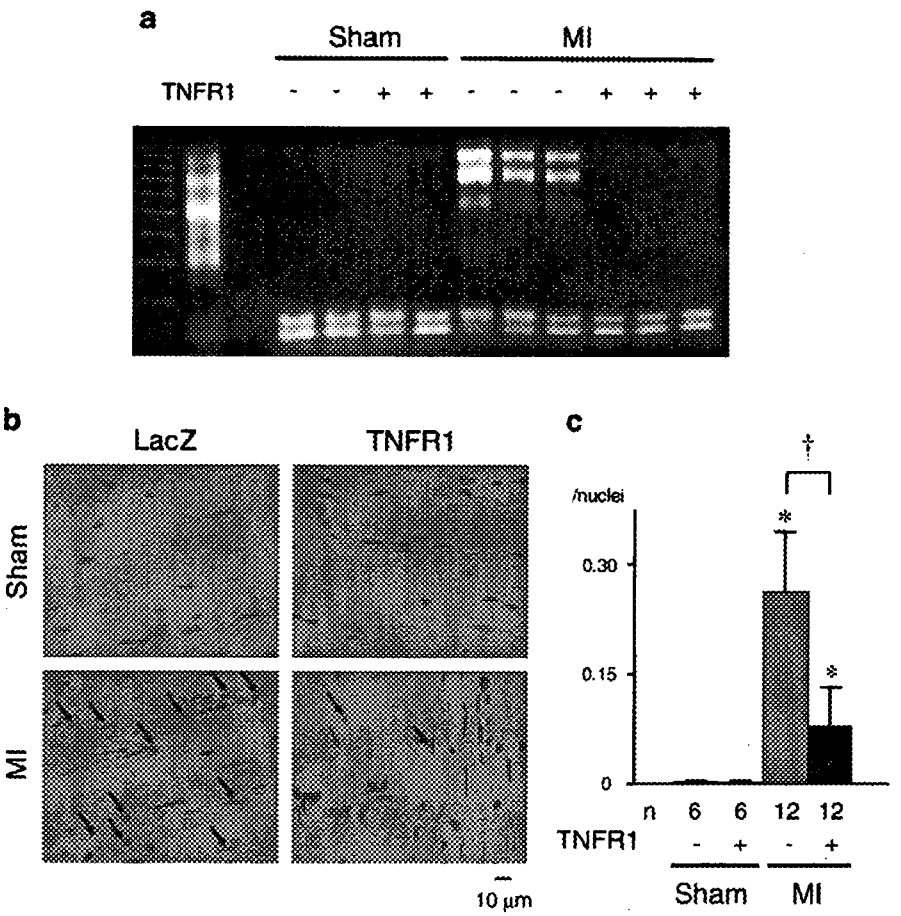

Fig. 3. Apoptosis assay in infarct myocardium on day 3 after MI: DNA laddering assay image (a), representative images of TUNEL staining (b), and summarized data for density of TUNEL-positive cells (c). Values are mean±SD. Arrows indicate TUNEL-positive cells; TNFR1 (−), pre-MI treatment with AdLacZ; TNFR1 (+), pre-MI treatment with AdTNFR1; Sham, sham-operated mice; MI, coronary ligated mice. *$p<0.05$ vs. Sham/LacZ mice, †$p<0.05$ vs. MI/LacZ mice.

receptors significantly increased the mortality after MI ($p<0.05$). The cause of death was classified as either congestive heart failure or ventricular rupture, because no mice died without congestion (pleural effusion and increased lung weight) or blood clot in the pericardial sac. Although mortality presumably due to congestive heart failure was not different between MI/LacZ and MI/TNFR1 mice (Fig. 2b), mortality due to ventricular rupture was significantly higher in MI mice treated with TNFR1 (Fig. 2c). To elucidate the mechanisms by which pre-MI TNFR1 treatment promotes ventricular rupture, the following studies were performed.

3.1.3. No differences in hemodynamic parameters or infarct size

Hemodynamic parameters and infarct size on days 3 and 14 after MI are summarized in Tables 1 and 2, respectively. Echocardiography revealed that both end-diastolic and end-systolic dimensions as well as non-infarct wall thickness increased progressively after MI, with significant decreases in fractional shortening and infarct wall thickness. These changes in echocardiographic parameters were not affected by treatment with TNFR1. Furthermore, infarct size was similar in MI/LacZ and MI/TNFR1 mice. Because neither

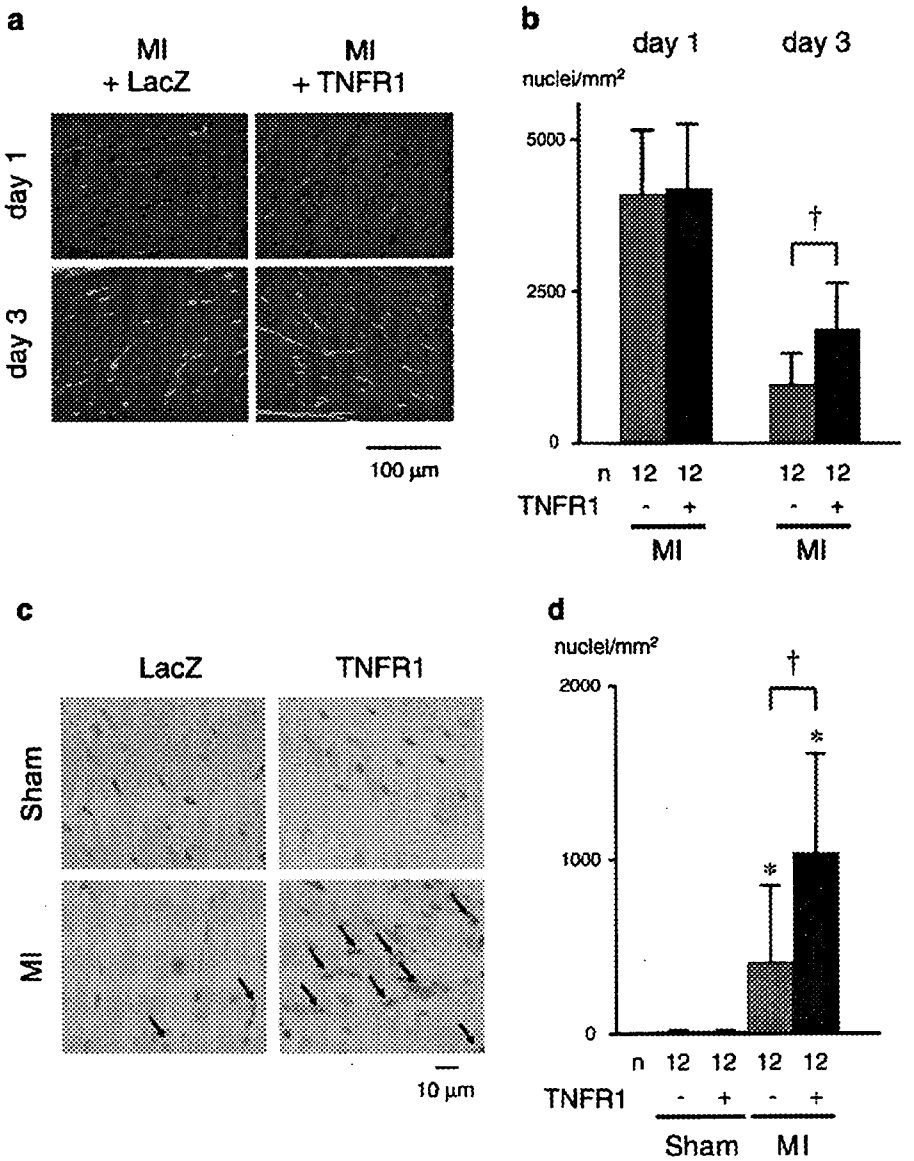

Fig. 4. Pathological analysis of the infarct myocardium: representative micrographs of hematoxylin–eosin staining (a), summarized data for total cell density on days 1 and 3 after MI (b), representative micrographs of immunohistochemical staining for mouse Mac-3 (c), and summarized data for density of Mac-3-positive cells on day 3 after MI (d). Values are mean±SD. Arrows indicate Mac-3-positive cells; TNFR1 (−), pre-MI treatment with AdLacZ; TNFR1 (+), pre-MI treatment with AdTNFR1; Sham, sham-operated mice; MI, coronary ligated mice. *$p<0.05$ vs. Sham/LacZ mice, †$p<0.05$ vs. MI/LacZ mice.

heart rate nor systemic blood pressure was affected by TNFR1 treatment, increased ventricular rupture in MI/TNFR1 mice was not attributable to increased afterload or wall stress.

3.1.4. Reduced apoptosis and retention of infiltrating macrophages

DNA laddering assay indicated that apoptosis, which increased substantially in infarct myocardium, was markedly decreased by TNFR1 treatment (Fig. 3a). TUNEL staining was performed to identify apoptotic cells on day 3. TUNEL-positive cells were mostly infiltrating mononuclear cells besides neutrophils and myocytes (Fig. 3b). As summarized in Fig. 3c, treatment with TNFR1 significantly reduced TUNEL-positive cells in infarct myocardium.

Hematoxylin and eosin staining was performed to evaluate infiltration of inflammatory cells. Marked infiltration of inflammatory cells was observed in infarct myocardium

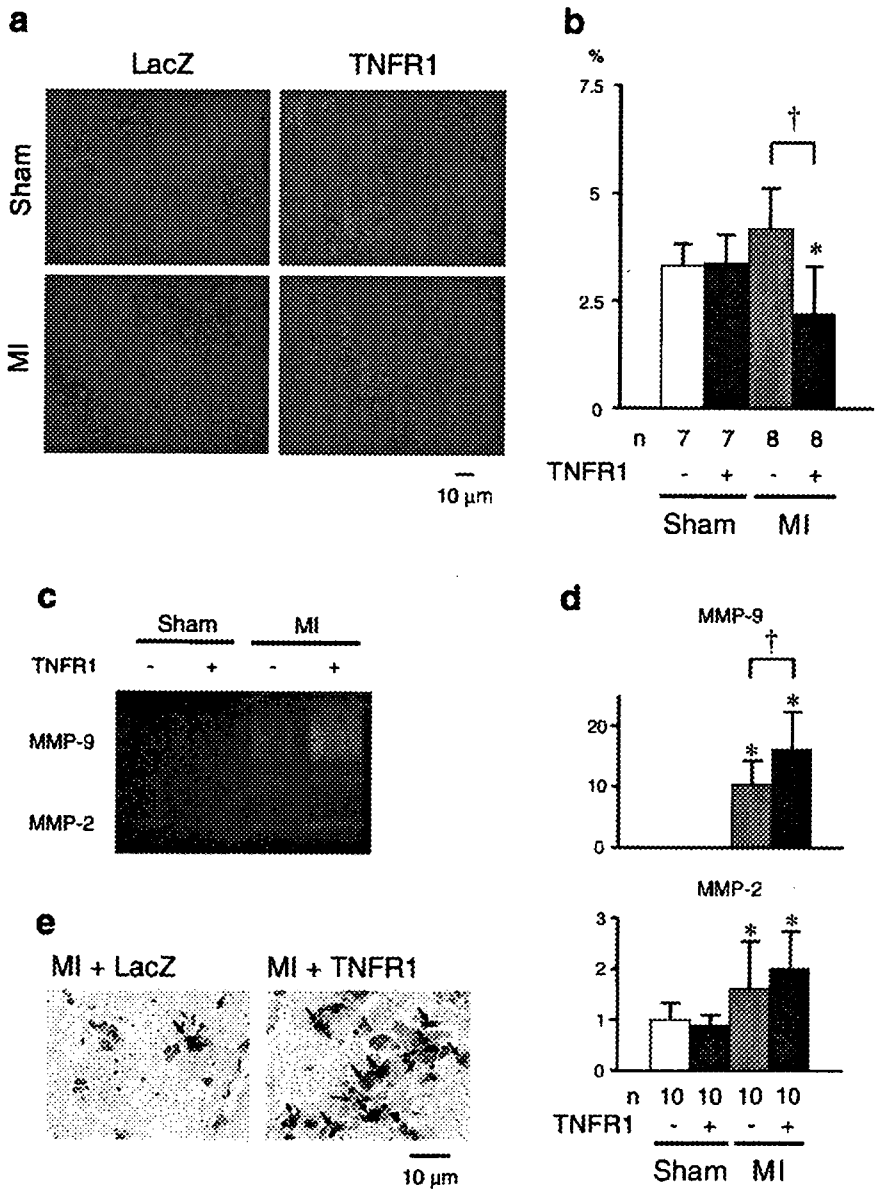

Fig. 5. Collagen volume analysis of the infarct myocardium on day 3 after MI: representative micrographs of Picrosirius red staining (a) and summarized data for collagen volume fraction (b). Gelatin zymography for MMP-2 and MMP-9 in infarct myocardium on day 3 after MI: representative gel (c) and summarized data for densitometric analysis (d). Each value is expressed as the ratio to the average of MMP-2 in Sham/LacZ mice. Double immunohistochemical staining for mouse Mac-3 and MMP-9 in infarct myocardium on day 3 after MI (e). Values are mean±SD. Arrows indicate both Mac-3- and MMP-9-positive cells; TNFR1 (−), pre-MI treatment with AdLacZ; TNFR1 (+), pre-MI treatment with AdTNFR1; Sham, sham-operated mice; MI, coronary ligated mice. *$p<0.05$ vs. Sham/LacZ mice, †$p<0.05$ vs. MI/LacZ mice.

on day 1, and subsequently subsided on day 3 (Fig. 4a). Although inflammatory cell infiltration was not significantly different between MI/LacZ and MI/TNFR1 mice on day 1, significantly more infiltrating cells remained in MI/TNFR1 myocardium on day 3, which might reflect reduced apoptosis by TNFR1 treatment (Fig. 4b). Immunohistochemical staining revealed that most of these retained infiltrating cells on day 3 were macrophages (Fig. 4c). As summarized in Fig. 4d, TNFR1 treatment significantly increased the number of macrophages in infarct myocardium on day 3.

3.1.5. Degradation of extracellular matrix with further activation of MMP-9

Collagen was visualized in LV cross-section using Picrosirius red staining (Fig. 5a). Collagen volume fraction was not affected by MI, but was significantly reduced in MI/TNFR1 mice on day 3 (Fig. 5b).

To further elucidate the mechanisms of reduced myocardial fibrosis in MI/TNFR1 mice, the activities of MMP-2 and -9 were evaluated in infarct myocardium on day 3 using gelatin zymography (Fig. 5c). The activities of MMP-2 and -9 increased significantly after MI (Fig. 5d). Treatment with soluble TNF receptors did not affect MMP-2 but significantly further activated MMP-9. Immunohistochemical staining identified macrophages as one of the major sources of MMP-9 in infarct myocardium (Fig. 5e).

Taken together, these results suggest that pre-MI treatment with TNFR1 prevents apoptosis of infiltrating cells in infarct myocardium, resulting in the retention of macrophages and further activation of MMP-9, which may further degrade and finally rupture the infarct myocardium.

3.2. Post-MI treatment protocol

3.2.1. Exacerbation of cardiac dysfunction and remodeling after MI

Post-MI treatment protocol was conducted to evaluate effects of TNFR1 on ventricular remodeling, because pre-MI treatment significantly increased ventricular rupture and precluded late phase analysis. In this study, 102 mice underwent coronary ligation, and 28 died within 7 days. The surviving mice ($n=74$) were randomly assigned to AdLacZ or AdTNFR1 injection on day 7. Four of 36 MI/LacZ and 9 of 38 MI/TNFR1 mice died of congestive heart failure by the end of 4 weeks after ligation (Fig. 6, $p=0.16$). None of the sham-operated mice died. Plasma levels of human TNFR1 3 weeks after inoculation with AdTNFR1 (or 4 weeks after MI or sham operation) were 71.1±28.5 (SD) μg/ml, which were similar to our previous report [18]. Percent infarct area was not different between MI/LacZ and MI/TNFR1 mice on day 28 (Table 3).

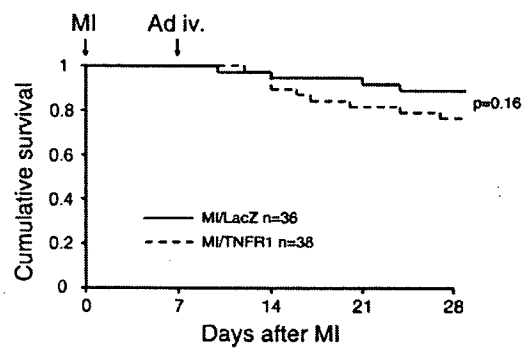

Fig. 6. Kaplan–Meier survival curves of coronary ligated mice with or without TNFR1 post-MI treatment.

Table 3
Characteristics of animal models (day 28)

	Sham/ LacZ	Sham/ TNFRI	MI/ LacZ	MI/ TNFR1
Echocardiographic data (under anesthesia)				
N	19	18	32	29
Heart rate (bpm)	465±11	461±13	471±16	467±14
LV EDD (mm)	3.9±0.3	4.0±0.3	5.6±0.3*	6.0±0.4*†
LV ESD (mm)	2.5±0.2	2.6±0.2	4.8±0.2*	5.3±0.5*†
Fractional shortening (%)	35.6±1.4	35.7±1.9	14.1±0.9*	11.7±1.9*†
Infarct wall thickness (mm)	–	–	0.29±0.03	0.29±0.03
Non-infarct wall thickness (mm)	0.78±0.04	0.76±0.05	0.95±0.06*	1.06±0.07*†
Hemodynamic data (Millar catheter, under anesthesia)				
N	6	6	12	11
Heart rate (bpm)	434±21	435±22	429±25	434±24
Mean aortic pressure (mm Hg)	81.8±4.3	80.5±4.6	78.3±4.3	79.2±4.5
LV EDP (mm Hg)	2.1±0.9	2.1±1.0	10.1±2.5*	14.5±3.3*†
LV$dP/dt_{max}$ (mm Hg/s)	7243±424	7084±422	5363±794*	4482±568*†
LV$dP/dt_{min}$ (mm Hg/s)	5047±274	4944±264	3864±602*	3219±424*†
Organ weight data				
N	19	18	32	29
Body wt (g)	42.0±2.1	41.9±2.4	40.7±2.5	40.6±3.1
Lung wt/Body wt (mg/g)	4.88±0.30	4.84±0.26	8.50±2.70*	10.13±2.78*†
Pleural effusion (%)	0	0	71.9	93.1
N	13	12	20	18
LV wt/Body wt (mg/g)	2.68±0.14	2.64±0.17	3.07±0.22*	3.33±0.29*†
N			12	11
Infarct area (%)	–	–	57.8±3.1	56.0±3.4*

LV, left ventricular; EDD, end-diastolic diameter; ESD, end-systolic diameter; EDP, end-diastolic pressure; wt, weight. Values are mean±SD. *$P<0.05$ vs. Sham/LacZ, †$P<0.05$ vs. MI/LacZ.

Echocardiography showed that cardiac dimensions of surviving mice on day 28 were significantly higher in MI/LacZ mice compared to Sham/LacZ or Sham/TNFR1 (Table 3). MI/TNFR1 mice showed significantly more cavity dilatation with exacerbation of contractile dysfunction compared with MI/LacZ. Pressure measurement with a Millar catheter showed no significant differences in heart rate and aortic blood pressure among 4 groups. However, LV end-diastolic pressure, which increased significantly in MI/LacZ mice, was further